Emilia Conti, Alessandro Scaglione, Giuseppe de Vito, Francesco Calugi, Maria Pasquini, Tommaso Pizzorusso, Silvestro Micera, Anna Letizia Allegra Mascaro and Francesco Saverio Pavone, “Combining Optogenetic Stimulation and Motor Training Improves Functional Recovery and Perilesional Cortical Activity”, Neurorehabilitation and Neural Repair (Volume 36, issue 2) pp. 107–118. Copyright © 2021 The Authors.

DOI: 10.1177/15459683211056656

Combined optogenetic stimulation and motor training improved functional recovery and perilesional cortical activity

Emilia Conti[1,2,3], Alessandro Scaglione[3], Giuseppe de Vito[2,4], Francesco Calugi[1,4], Maria Pasquini[5,6], Tommaso Pizzorusso[1,4], Silvestro Micera[5,6], Anna Letizia Allegra Mascaro[1,2*], Francesco Saverio Pavone[2,3,7]

1 Neuroscience Institute, National Research Council, Pisa, Italy

2 European Laboratory for Non-linear Spectroscopy University of Florence, 50100 Florence, Italy

3 Department of Physics and Astronomy, University of Florence, 50100 Florence, Italy

4 Department of Neurofarba, University of Florence, 50100 Florence, Italy

5 The BioRobotics Institute and Department of Excellence in Robotics and AI, Scuola Superiore Sant'Anna, Pisa, Italy

6 Bertarelli Foundation Chair in Translational NeuroEngineering, Center for Neuroprosthetics and Institute of Bioengineering, Ecole Polytechnique Federale de Lausanne (EPFL), Lausanne, Switzerland

7 National Institute of Optics, National Research Council, 50100 Florence, Italy

*Corresponding author: Anna Letizia Allegra Mascaro Via Moruzzi 1, 56124 Pisa, Italy

e-mail: allegra@lens.unifi.it

telephone number: 05524762504

Abstract

Background: An ischemic stroke is followed by the remapping of motor representation and extensive changes in cortical excitability involving both hemispheres. Although stimulation of the ipsilesional motor cortex, especially when paired with motor training, facilitates plasticity and functional restoration, the remapping of motor representation of the single and combined treatments is largely unexplored.

Objective: We investigated if spatio-temporal features of motor-related cortical activity and the new motor representations are related to the rehabilitative treatment or if they can be specifically associated to functional recovery.

Methods: We designed a novel rehabilitative treatment that combines neuro-plasticizing intervention with motor training. In detail, optogenetic stimulation of peri-infarct excitatory neurons expressing Channelrhodopsin 2 was associated with daily motor training on a robotic device. The effectiveness of the combined therapy was compared with spontaneous recovery and with the single treatments (i.e. optogenetic stimulation or motor training).

Results: We found that the extension and localization of the new motor representations are specific to the treatment, where most treatments promote segregation of the motor representation to the peri-infarct region. Interestingly, only the combined therapy promotes both the recovery of forelimb functionality and the rescue of spatio-temporal features of motor-related activity. Functional recovery results from a new excitatory/inhibitory balance between hemispheres as revealed by the augmented motor response flanked by the increased expression of parvalbumin positive neurons in the peri-infarct area.

Conclusions: Our findings highlight that functional recovery and restoration of motor-related neuronal activity are not necessarily coupled during post-stroke recovery. Indeed the reestablishment of cortical activation features of calcium transient is distinctive of the most effective therapeutic approach, the combined therapy.

Keywords: photothrombotic stroke; optogenetic stimulation; motor training; calcium imaging; rehabilitation

Introduction

Ischemic injuries within the motor cortex result in functional deficits that may profoundly alter patients' quality of life. Survivors are often chronically impaired with long-term disability[1]. To regain sensory and motor functions after stroke, spared neural circuits must reorganize[2-4]. Multiple strategies have been developed to enhance neural rewiring which dramatically improved functional recovery[4] including pharmacological treatment, motor training, and brain stimulation. Among them, cortical neuromodulation techniques, such as transcranial magnetic stimulation (TMS) and transcranial direct current stimulation (tDCS), represent a promising non-invasive approach to improve cortical remapping. Nevertheless, these treatments can induce diffuse and non-specific activation in mixed neuronal populations[5-7], revealing the necessity for more targeted therapies. With the emergence of optogenetics, specific neuronal populations can be activated or inhibited achieving high temporal and spatial precision[8-11]. Recently, optogenetics has been proficiently used to selectively modulate the excitatory/inhibitory balance of brain circuits affected by a stroke lesion[12,13]. Repeated optogenetic neuronal stimulation of the ipsilesional hemisphere induced a significant improvement in neurovascular coupling response[14]. Furthermore, chronic optogenetic stimulation of the entire cortical mantle promoted behavioral recovery associated with the formation of new and stable thalamocortical synaptic boutons[15]. Nevertheless, information on the remapping of motor representation and motor-related cortical activation following optogenetic stimulation is largely unexplored. Further, no study investigated how stimulation-induced cortical remapping correlates with functional recovery.

When combined with motor training, cortical stimulation creates a pro-plasticizing milieu where spared neurons are more susceptible to experience-dependent modifications[4,16,17].

Though several studies investigated the effect of combining neuronal modulation, such as TMS[18-20] and tDCS[21-23], with robotic training, results are contradictory. Up to now, whether the combination of ipsilesional neuronal stimulation and physical training promotes motor recovery is still unknown. Further, though it is established that the combination of neuronal modulation and motor training plays a key role in post-stroke recovery, no investigation has yet addressed if possible physical improvement is supported by alterations in motor maps and in the distributed motor-related cortical activation.

Here, we designed a light-based stimulation protocol of peri-infarct excitatory neurons as a rehabilitative approach to achieve functional recovery, measured in a behavioral test different from the rehabilitation task.

Our hypothesis is that combination of optogenetic stimulation of peri-lesioned cortex and repetitive motor training of the affected forelimb boosts post-stroke recovery by promoting the establishment of a new excitatory/inhibitory balance between hemispheres. To dissect cortical remapping in motor-related neuronal activity in peri-infarct area we took advantage of wide-field fluorescence imaging over the affected hemisphere. We found that longitudinal optogenetic stimulation restored forelimb functionality whereas motor-related functional activity did not recover. However, coupling optogenetic stimulation with longitudinal motor training of the impaired forelimb on a robotic platform halved the time required for a full recovery of forelimb function compared to optogenetic stimulation only. Furthermore, the rapid behavioral recovery was associated with the restoration of temporal features of calcium transient such as peak amplitude and slope. The analysis of motor-related activation maps in mice with combined therapy identified the peri-infarct area as the region of the cortex mostly involved in motor task. Finally, the combined treatment promoted the restoration of an interhemispheric balance between the two hemispheres, revealed by an increase of expression

of Parvalbumin positive cells in the peri-infarct area, and plasticity marker, GAP43, both in per-infarct neurons and in contralesional hemisphere's fibers.

Methods

Mice

All procedures involving mice were performed in accordance with regulations of the Italian Ministry of Health authorization n. 871/2018. Mice were housed in clear plastic cages under a 12h light/dark cycle and were given ad libitum access to water and food. We used a transgenic mouse line, C57BL/6J-Tg(Thy1GCaMP6f)GP5.17Dkim/J, from Jackson Laboratories (Bar Harbor, Maine USA). This transgenic mouse line expresses the green fluorescent indicator in a subset of excitatory neurons, i.e. pyramidal neurons[24]. Mice were identified by earmarks and numbered accordingly. Animals were randomly divided into 5 groups. Each group contained comparable numbers of male and female mice (weighing approximately 25g). Age of mice (ranging from 6 to 8 months old) was consistent between groups. Sample size (25 mice) was chosen according to a priori power analysis (Supplementary Materials, Mice subsection).

Experimental design:

Animals were distributed in 5 groups as follows: Sham n=6; Stroke n=4; Optostim n=4; Robot= 7; Optostim+Robot (abbreviated in OR) n= 4 (Supplementary Figure 2).

- The Sham group consists of 6 healthy mice. During surgery instead of induced photothrombosis we intraperitoneally injected saline and then we illuminated the primary motor cortex (+1.75 ML and +0.50 AP). We then intracranially injected saline in the sensory cortex (+1.75 ML and -0.75 AP). After 5 days of recovery from surgery mice performed 5 days of motor assessment on the robotic platform in order to investigate cortical activation during a motor task in healthy conditions.
- The Stroke group consists of 4 mice. At the beginning of the protocol we evaluated forelimbs use via Schallert cylinder test. We induced a focal stroke in the primary motor cortex (+1.75

ML and +0.50 AP). During the same surgery we intracranially injected saline in the sensory cortex (+1.75 ML and -0.75 AP). Two days after surgery we performed behavioral tests to identify alteration in forelimb use consequent to stroke. We performed behavioral experiments at the end of each week to longitudinally investigate spontaneous recovery. After 5 days of recovery from surgery we stimulated Stroke mice, though not expressing Channelrhodopsin 2 (ChR2), with a blue laser for 20 days to evaluate possible artifacts due to repeated laser stimulation. After 25 days of spontaneous recovery mice performed 5 days of motor assessment on the robotic platform in order to investigate motor-related cortical activation. 30 days after stroke mice were perfused.

- The Optostim group consists of 4 mice. At the beginning of the protocol we evaluated forelimbs use via Schallert cylinder test. We induced a focal stroke in the primary motor cortex. During the same surgery we intracranially injected an adeno associated virus (AAV9-CaMKII-ChR2-mCherry) to induce the expression of ChR2 in the sensory areas. Two days after surgery we performed behavioral tests to identify alteration in forelimb use consequent to stroke. After 5 days of recovery from surgery mice began the rehabilitation paradigm consisting in 20 days of optogenetic stimulation of the peri-infarct area. 25 days after photothrombosis, mice performed 5 days of motor assessment on the robotic platform in order to investigate motor-related cortical activation. At the end of each week of rehabilitation we performed behavioral experiments to longitudinally investigate mice recovery. 30 days after stroke mice were perfused.
- The Robot group consists of 7 mice. At the beginning of the protocol we evaluated forelimbs use via Schallert cylinder test. We induced a focal stroke in the primary motor cortex. During the same surgery we intracranially injected an adeno associated virus (AAV9-CaMKII-ChR2-mCherry) to induce the expression of ChR2 in the sensory areas. Two days after surgery we performed behavioral tests to identify alteration in forelimb use consequent to stroke. After 5 days of recovery from surgery mice began the rehabilitation paradigm consisting in 20 days of

robotic training. At the end of each week of rehabilitation we performed behavioral experiments to longitudinally investigate mice recovery. 30 days after stroke mice were perfused.

- The Optostim+Robot group consists of 4 mice. At the beginning of the protocol we evaluated forelimbs use via Schallert cylinder test. We induced a focal stroke in the primary motor cortex. During the same surgery we intracranially injected an adeno associated virus (AAV9-CaMKII-ChR2-mCherry) to induce the expression of ChR2 in the sensory areas. Two days after surgery we performed behavioral tests to identify alteration in forelimb use consequent to stroke. At the end of each week of rehabilitation we performed behavioral experiments to longitudinally investigate recovery. After 5 days of recovery from surgery mice began the rehabilitation paradigm consisting in 20 days of robotic training followed by optogenetic stimulation of the peri-infarct area. 30 days after stroke mice were perfused.

Surgical procedures

Mice were injected with a Rose Bengal solution (0.2 ml, 10 mg/ml solution in Phosphate Buffer Saline (PBS)). Five minutes after intraperitoneal injection a white light from an LED lamp was focused with a 20X objective to illuminate the primary motor cortex (M1) for 15 min inducing unilateral stroke in the right hemisphere. During the same procedure, we delivered 0.5 µl of AAV9-CaMKIIa-hChR2(H134R)-mCherry ($2.48*10^{13}$ GC/mL) 600µm deep inside the cortex at -0.75 AP, +1.75 ML. For further information see Supplemental Material.

Robotic Platform

Animals were trained by means of the M- Platform[25,26], which is a robotic system that allows mice to perform a retraction movement of their left forelimb. Motor rehabilitation consists in a pulling task: first animal forelimb is passively extended by the linear actuator of the platform and then the animal has to pull back forelimb up to the resting position. Motor training is composed of 15 movements and after each movement the animal receives a liquid reward. For further information see Supplemental Material.

Optogenetic stimulation

Daily optogenetic stimulation was performed on head-fixed awake mice by employing a 473 nm laser delivering 5 Hz, 10ms light pulses. Laser power, ranging from 0.2 to 0.8 mW, was daily adjusted according to the increment of the transfected area and the progressive lowering of stimulation threshold over the weeks. For further information see Supplemental Material.

Statistical analysis

Statistical analysis was performed using OriginPro software (OriginLab Corporation), and results were considered statistically significant with a p value <=0.05. All the statistical comparisons were performed simultaneously across all experimental groups.

For the statistical analysis of the Schallert cylinder data we performed a repeated-measure ANCOVA analysis on raw data (without normalization with pre-stroke asymmetry index) using "Group", "Week" and their interaction as qualitative variables, "pre-stroke asymmetry index" as a quantitative variable and the animal identifier as designator. Post-hoc analysis was then performed by computing linear contrasts for all pairwise comparisons among estimated marginal means for the variables "Week" and "Group." Multiplicity adjustment was carried out with Tukey's method. In case where different timepoints of the same group were compared, a one-way repeated measure ANOVA with factor TIME was used.

For calcium, forces and immunohistochemical analysis, a one-way ANOVA was used, with factor GROUP. For all ANOVAs that were statistically significant, multiple comparison among groups, or time points, were assessed using Tukey HSD test. For information regarding Schallert cylinder test, wide-field microscope, and image, forces, and immunohistochemical analysis see Supplemental Material.

Results

Peri-infarct optogenetic stimulation restores forelimb function but not cortical activation features

The main goal of this study is to find a neuronal substrate of functional recovery within the distributed motor-related cortical activity. To this aim, we compared behavioral and calcium imaging data from mice receiving three different treatments, optogenetic stimulation, motor training and a combination of them. First, the efficacy of repeated optogenetic stimulation of peri-infarct excitatory neurons was tested in stroke mice. A photothrombotic stroke was induced on the M1 of the right hemisphere in Thy1-GCaMP6f mice (Supplementary Figure 1A). We developed a rehabilitation protocol based on longitudinal optogenetic stimulation of peri-infarct excitatory neurons expressing Channelrhodopsin 2 (ChR2, Figure 1A and Supplementary Figure 1B-D). Optogenetic stimulation was performed daily and consisted of three successive 30-sec laser stimulation trains, separated by 1-min rest intervals (Figure 1B). The optogenetic therapy lasted 4 weeks starting 5 days after stroke. We divided our sample into 3 groups (Figure 2A, Supplementary Figure 2 and Experimental design Materials and Methods section): Sham (healthy mice, no stroke), Stroke (stroke, spontaneous recovery), Optostim (stroke, optogenetic rehabilitation). During the last week of our investigation mice performed 5 days of motor assessment in order to evaluate motor-related cortical activity (Figure 1C).

We longitudinally estimated functional recovery of forelimb functionality as a measure of forelimb-use asymmetry by performing Schallert cylinder test at the end of each week of treatment. In detail, the test quantifies the asymmetry index (A.i.) as the relative number of weight-bearing touches with one or both paws when the mouse descends and rears during the exploration of the cylinder walls. The longitudinal evaluation of the asymmetry index of spontaneously recovered mice (Stroke group), significantly different to pre-stroke conditions from the acute phase after stroke (2dpl), highlights the preferential use of the unaffected forelimb indicating the absence of spontaneous recovery up to 4 weeks after the insult (Figure

2B). Conversely, a full recovery of forelimb function was achieved after 4 weeks of daily optogenetic stimulation (Optostim group, Figure 2B). Indeed, the comparison of the asymmetry index at different time points within the Optostim group highlights that the use of forelimb became significantly different with respect to the acute phase after stroke (2dpl) after 4 weeks of treatment.

We then assessed if behavioral recovery was associated with specific features of motor-related cortical functionality. To this aim, we performed wide-field calcium imaging of the affected hemisphere on GCaMP6f mice during the execution of a pulling task within a robotic device, the M-Platform[25,26]. The M-Platform was previously integrated with a custom-made wide-field mesoscope to perform calcium imaging of motor-related activity and optogenetic stimulation[27-30]. This robotic device allowed a detailed assessment of motor-related cortical activation during an active forelimb pulling task.

To evaluate possible spurious activation of ChR2 expressing neurons induced by the blue LED used for calcium imaging, we performed control experiments in Thy-GCaMP6f mice with or without ChR2 injection while performing 4 weeks of motor training. No significant differences in the peak amplitude and slope of calcium transients were observed between $ChR2^{+}$ mice and $ChR2^{-}$ (Supplementary Figure 3A), demonstrating that ChR2 stimulation induced by the imaging LED was negligible or absent.

We then analyzed the spatial extension of motor representation in the ipsilesional hemisphere (Supplementary Figure 3B) by overlapping the movement-triggered activation maps obtained for each day of training. This comparison showed a segregated activation in healthy mice, whereas in Stroke and Optostim mice the maps covered most of the affected hemisphere, up to the caudal regions of the cortex (such as retrosplenial and visual areas Figure 2C-D), as quantified by analyzing distance from bregma of motor-related map's centroid (Figure 2E). Then, we explored the possibility that temporal features of activation might be correlated with

functional recovery in the Optostim group. To this aim we investigated amplitude and slope of calcium transient as an estimate of the extent and the velocity of the rising phase of neuronal activation during movement execution. However, by analyzing the fluorescence transients averaged from the region of maximum calcium activation during active pulling, we observed no significant differences in amplitude and timing in Optostim mice compared to spontaneously recovering Stroke mice (Figure 2F). These results demonstrate that, even though recovery of forelimb function can be achieved by optogenetic stimulation alone, the spatiotemporal features of motor-related cortical activity in the ipsilesional hemisphere did not recover to pre-stroke conditions.

Combining optogenetic stimulation with motor training boosts the functional recovery and is associated with reshaping of motor-related activation maps and restoration of temporal features of calcium transients

In a previous study, we showed that a combined rehabilitation protocol of pharmacological inactivation and motor training was beneficial to achieve a proficient functional recovery[31]. We hypothesized if an even more effective recovery could be achieved by coupling optogenetic stimulation to longitudinal motor training of the affected forelimb on the M-platform. Thus, a rehabilitation protocol combining daily training on the M-Platform and optogenetic stimulation was tested (OR group, Figure 3A and Supplementary Figure 2). We choose to sequentially perform motor training and optogenetic stimulation of the peri-infarct cortex to avoid a potential bias on fluorescence signal during motor training (calcium imaging) due to the previous excitation of the cortex. The combined treatment was applied daily from the acute phase (5 days after stroke) up to 4 weeks after stroke. The OR group was then compared to healthy mice (Sham group), spontaneous recovery (Stroke group), and motor exercise alone (Robot group). Training induced a progressive modulation of the force transients measured on the M-Platform during active pulling of the affected forelimb. A small reduction in amplitude and full-width

half maximum (FWHM), though not statistically significant, was seen both in OR and Robot mice (Supplementary Figure 3C). In addition, the progressive decrease of time-to-target visible in mice with combined therapy was in line with previous findings in robot-treated stroke mice[26]. We then evaluated alterations in spontaneous forelimbs use on Schallert cylinder test. In accordance with Spalletti and colleagues[32], motor training alone was not able to restore pre-stroke performances (Figure 3B). Indeed by comparing the Asymmetry index (A.i). of Stroke and Robot mice no significant differences were revealed between groups. Conversely, the comparison of A.i. at different time points with respect to the acute phase after stroke (◊), highlights that OR mice recovered forelimb functionality already on the second week of rehabilitation (Figure 3B), thus supporting the hypothesis that combined rehabilitation boosts recovery. Indeed, as emerges from the comparison with pre-stroke condition (*), the use of forelimb is shifted towards the non-paretic limb in the acute phase after stroke (2days post-lesion and after I week of treatments). During the rehabilitation period (II-IV weeks of treatment) the asymmetry index was recovered in OR mice to pre-stroke levels, significantly different (#) from spontaneously recovered mice (III and IV weeks of treatment).

We wondered if this fast behavioral improvement due to the combined treatment was mirrored into specific spatiotemporal features of motor-related cortical activity. Examples of temporal sequences of pulling-evoked cortical activation are shown in Figure 3C, together with the associated motor representations (i.e. the thresholded motor-related maps, see Supplementary Materials and Methods section) on the fourth weeks after stroke (Figure 3D). The motor representations of both Robot and OR groups partially resemble the Sham group, with a similarly short distance of the centroid of the motor representation to bregma (Figure 3E). Moreover, as shown in figure 3D the region of maximum activation is confined to a segregated region of the cortex in the peri-infarct area. Conversely, the motor representation of the Stroke group (Figure 2D) is shifted more caudally and is divided into two regions diffusing from the

sensory to the visual areas of the cortex. This means that daily motor training promotes the segregation of motor representation to the peri-infarct area. Interestingly, after combined therapy, the motor representation largely overlaps the caudal portion of the secondary motor cortex, according to the Paxinos and Franklin Mouse Brain Atlas[33]. We further investigated how the temporal profiles of calcium transients averaged over the motor representation area were altered after combined rehabilitation. Amplitude and slope in mice treated with motor training alone (Robot group) were comparable to spontaneous recovery (Stroke group). Conversely, the synergic effect of combined rehabilitation promoted the reestablishment of these salient features of calcium transient in peri-infarct area (Figure 3F, G). This positive trend towards pre-stroke conditions (Sham group), though not significantly different, started from the second week of rehabilitation in OR mice (Supplementary Figure 3D). The pronounced increment in peak amplitude and slope of calcium transient in combined rehabilitated mice became comparable to healthy condition after 4 weeks of combined treatment.

The modulation of cortical motor-related activity from excitatory neurons could be associated with a new excitatory/inhibitory balance[14] potentially compensating detrimental consequences of stroke[34]. We thus evaluated the density of parvalbumin-positive (PV^+) cells throughout all cortical layers of the peri- and contra-lesional cortices (Figure 3H). In the peri-infarct region, a small but not significant increase of PV^+ cell density was induced by the single treatments (Optostim and Robot, Figure 3I) with respect to spontaneous recovery mice (Stroke group). Interestingly, the PV^+ cell density is significantly higher in peri-infarct cortex of mice with combined therapy (OR group) compared to non-treated (Stroke) animals (Figure 3I). Conversely, no significant differences were observed in the contralesional hemisphere in all groups (Supplementary Figure 4A). Together with the increased motor-related activation levels in pyramidal cells, these results suggest that the synergic effect of combined rehabilitation could

promote the establishment of a new excitatory/inhibitory equilibrium in the peri-infarct and contralesional hemispheres.

Functional recovery is associated with an increased expression of GAP43

To further identify molecular targets associated with functional recovery, we tested the presence of plasticity markers in the lesioned and contralesional cortex by immunohistochemical analysis. We examined the expression of the growth-associated protein 43 (GAP43), a plasticity marker involved in synaptic turnover and reorganization after stroke[3,32,35]. While after optogenetic stimulation (Optostim group) or motor training (Robot group) GAP43 expression levels were comparable to spontaneously recovered mice (Stroke group), combined rehabilitative treatment promoted a massive expression of this neuronal plasticity marker in the peri-infarct region (Figure 4A). Though in the contralesional hemisphere no differences in $GAP43^+$ cells were observed between groups (Supplementary Figure 4B), an increase in number and length of $GAP43^+$ fibers was present in the homotopic areas on the contralesional hemisphere after all treatments (Optostim, Robot, and OR groups; Figure 4B). Nevertheless, only the combined treatment (OR group) showed significantly different density of $GAP43^+$ neurites compared to spontaneously recovered mice (Stroke group). This result demonstrate that perilesional stimulation and motor training synergistically enhance the density of $GAP43^+$ neurites in distal regions functionally related to the stroke core, which is possibly associated to axonal sprouting[36-38] or dendritogenesis[39,40].

Taken together, the histological analysis shows that behavioral recovery and the associated cortical remapping induced by combined rehabilitation are supported by a plasticizing milieu promoted by the synergic effect of ipsilesional neuronal stimulation and repetitive motor training.

Discussion

The present study aimed at understanding the neuronal correlate of functional recovery. By taking advantage of recent advancements in optical tools, including *in vivo* fluorescence imaging and optogenetics, to characterize critical features of plasticity, repair and recovery after stroke[31,41-45], we investigated the motor-related distributed cortical activity in several rehabilitation paradigms. Among the treatments, both the optogenetic stimulation of perilesional excitatory neurons (Optostim group) and the combined therapy with optogenetic stimulation and motor training of the paretic forelimb (OR group) led to functional recovery. However, the novel combined rehabilitation paradigm validated here led to the behavioral recovery of forelimb functionality, significantly faster than optogenetic stimulation alone. Moreover the combinatory treatment induces the restoration of spatiotemporal features of cortical activity to pre-stroke levels. Based on these results our hypothesis is that functional recovery is supported by the establishment of a new excitatory/inhibitory balance between hemispheres, revealed by the augmented cortical motor response flanked by increased expression of PV+ neurons in the peri-infarct cortex.

We first assessed the consequences of the optogenetic treatment consisting of 4 weeks of daily perilesional stimulation. In this work we assess the motor functionality through Schallert cylinder test only in order to evaluate forelimb use preference after the insult and in different rehabilitative therapies, however in future studies a combination of different motor tests will better evaluate different aspects of functional recovery such as fine motor control and forelimb dexterity. Previous works demonstrated the efficacy of post-stroke optogenetic stimulation on both the peri-infarct cortex[14,15] and striatum[46] in promoting the recovery of forelimb sensory-motor abilities. In agreement with these findings, we revealed a remarkable improvement of forelimb functionality after 4 weeks of optogenetic stimulation of the peri-lesioned excitatory neurons. Our data also agree with the observation by Tennant and colleagues that even if optogenetic rehabilitative treatment enhanced the restoration of somatosensory cortical circuit

function, the cortical area responsive to optogenetic stimulation and the peak of motor-related cortical activity after 4 weeks of treatment were not fully recovered to pre-stroke levels. Accordingly, our observations indicate that our optogenetic treatment *per se* does not recover pre-stroke spatio-temporal features of motor-related cortical activation. Indeed, a diffuse activation involving regions across the entire lesioned hemisphere is observed during active pulling of the paretic forelimb. In addition to these diffuse motor representation motor-related cortical activation profiles of the Optostim group have lower amplitude compared to pre-stroke conditions. Thus, our results support the hypothesis that optogenetic stimulation of excitatory spared neurons counteracts the increased excitability of the contralesional M1, thus balancing the excessive inhibitory drive onto the ipsilesional cortex. Taken together these results highlight that the restoration of pre-stroke features of cortical activity is not an essential requisite to achieve the recovery of forelimb functionality.

On the other hand, although Robot trained mice did not achieve a functional recovery, their motor-related map is segregated to the sensorimotor regions, similarly to healthy mice (Sham group). Nevertheless, longitudinal motor training alone did not restore pre-stroke features of calcium transient. These results confirm that motor training alone promotes a task-specific motor improvement as previously shown by Spalletti and collaborators[32], which is allegedly associated to the stabilization of motor representation[47].

Finally, the combined rehabilitative treatment triggered a synergic effect that connects behavioral improvement to recovery of pre-stroke motor-related cortical activation. Indeed, the combination of cortical stimulation and motor training induces a fast restoration of the forelimb function towards healthy conditions, as measured via asymmetry index analysis in the Schallert cylinder test. At the same time, flanking the stimulation with repeated exercise leads to both confinement of motor representations and restoration of temporal features of motor-related calcium transient in the peri-lesioned cortex, towards the pre-stroke condition. The strong

involvement of spared neurons in the secondary motor cortex revealed in the motor representation of OR mice could play a leading role in regaining functional recovery. Our results highlight the synergic effect of the combined rehabilitation since counterbalancing the contralesional inhibition of peri-infarct cortex by optogenetic stimulation could enable the stabilization of spared circuitry achieved by longitudinal motor training.

We showed an increase in motor-related cortical activation mediated by excitatory cells in the peri-infarct area of OR mice compared to single treatments (Optostim and Robot groups) and spontaneous recovery (Stroke group). Together with the higher levels of parvalbumin expression, these results provide evidence that the combined treatment might promote the restoration of an excitatory/inhibitory balance in the peri-infarct cortex similar to pre-stroke conditions. It has been previously demonstrated that parvalbumin expressing neurons may contribute to long-range GABAergic projections [48,49]. Moreover, Rock and collaborators [50] recently found a direct inhibitory pathway made up of PV neurons connecting corresponding cortical areas (i.e. motor, auditory, and visual cortices) in the two hemispheres through the corpus callosum. In our study, the increase of inhibitory cells in the peri-infarct cortex may counteract the iper-inhibition exerted by the healthy hemisphere through long-range cortico-cortical projections. Finally, previous studies demonstrated that modulation in parvalbumin expression is associated with achievement of skilled ability in motor task[51]. Our results are in line with what observed by Swanson and Maffei, who shows that PV expression is stabilized to higher expressions level once motor performance is saturated. In our study, the small increment of PV^+ cells observed in the Robot group is strongly enhanced in OR mice. The combination of motor training with optogenetic stimulation further stimulates the inhibitory activity in the perilesional cortex.

The behavioral improvement is supported by the long-lasting expression of growth-associated factors in the perilesional area, as demonstrated by the increased number of cells expressing

GAP43. It was previously demonstrated that this growth-associated factor promotes cortical remapping[3], axonal sprouting[3,34,35], and dendritogenesis[39,40] after stroke. This result extends previous findings by Cheng and collaborators showing that perilesional optogenetic stimulation after stroke promotes a global increase in GAP43 expression involving both hemispheres[14]. Also, our findings are in agreement with Spalletti and collaborators[32] showing that a combined rehabilitative treatment leading to functional recovery promotes an increase of plasticity markers expression. The recovery of the excitatory/inhibitory balance could be further supported by the axonal sprouting in the contralesional cortex, where a substantial number of $GAP43^+$ fibers were detected, particularly in combined rehabilitated mice. The increment of $GAP43^+$ cells in the peri-infarct area, in combination with $GAP43^+$ axons in the contralesional region, suggests the arise of transcallosal axonal sprouting from the ipsilesional hemisphere.

One of the main results of the present study is that restoration of motor functionality can occur without recovery of spatiotemporal features of motor-related cortical activation that characterize pre-stroke mice, as in Optostim mice. On the other hand, segregation of motor representation is not necessarily entangled with functional recovery, as in Robot mice. These findings suggest that rehabilitation strategies for functional recovery might not essentially aim at the restoration of pre-stroke features of motor-related activity, as observed in a recent work by Cecchini and collaborators[30]. Nevertheless, the reestablishment of pre-stroke activation transients was a distinguished feature of the most efficient therapeutic approach, the combined therapy. In accordance with our previous findings[31] on a different combined rehabilitation paradigm, this study supports the hypothesis that the restoration of pre-stroke temporal features could be an important biomarker of the functional recovery.

To conclude, we developed a post-stroke rehabilitation therapy that exploits the synergic effect of peri-infarct optogenetic excitation and repetitive motor training to promote the stabilization of a new excitatory/inhibitory balance between hemispheres resulting in the recovery of

forelimb functionality and spatio-temporal features of motor-related calcium transient. This study highlights how the outcome of rehabilitation therapies depends on a balance between stabilization of peri-infarct circuitry and fostering of cortical plasticity.

Acknowledgments

We thank K. Deisseroth for opsin plasmids. We thank Matteo Caleo, Cristina Spalletti and Claudia Alia for very useful discussion about the manuscript.

Sources of Funding

This project has received funding from the H2020 EXCELLENT SCIENCE - European Research Council (ERC) under grant agreement 692943 BrainBIT. In addition, it was supported by the European Union's Horizon 2020 Research and Innovation Programme under Grant Agreements 785907 (HBP SGA2), and 654148 (Laserlab-Europe).

Declaration of Interests

The authors declare no competing interests.

Author Contributions

E.C., A.L.A.M. and F.S.P. conceived the study. E.C., A.L.A.M. and F.C. performed experiments. E.C., A.S., G.d.V., M.P., processed data. F.S.P., T.P. and S.M. obtained funding support. E.C. and A.L.A.M. wrote the paper. All authors approved the paper.

Figures

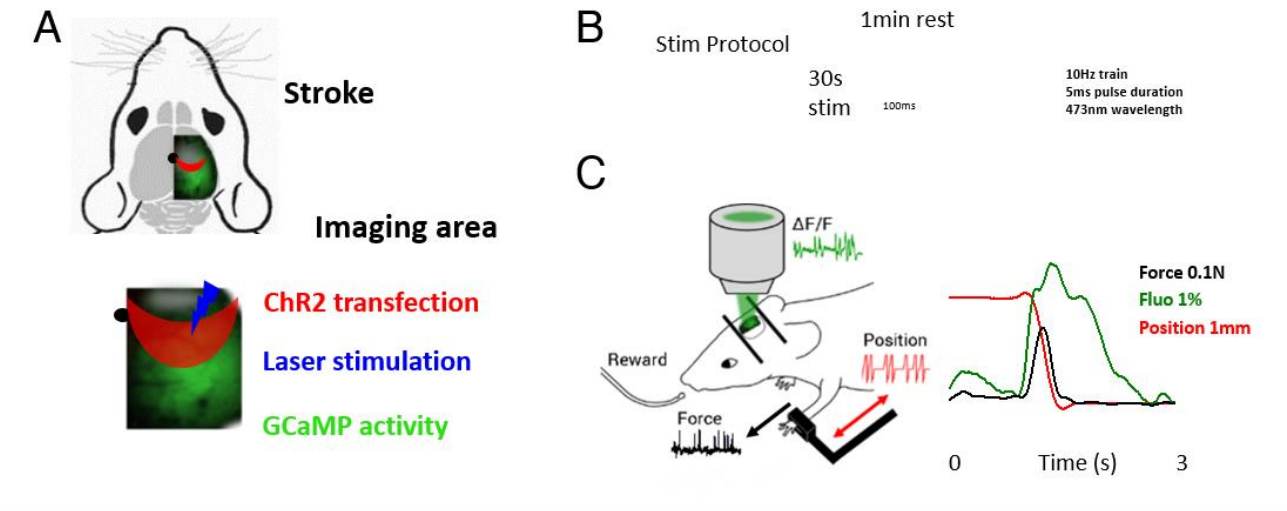

Figure 1. Experimental design: (A) Field of view graphical representation: ChR2-expressing neurons (red area) are stimulated by blue laser. Cortical activity is revealed in the right hemisphere during motor assessment. Grey cloud represents stroke core, black dot represents bregma. (B) Stimulation paradigm consisting of 3 stimulation train separated by 1-min rest intervals. (C) Graphical representation of M-Platform for motor assessment. Graph on the right shows an overlap of simultaneously recorded traces (Force, Fluorescence and Position) of an exemplary retraction movement.

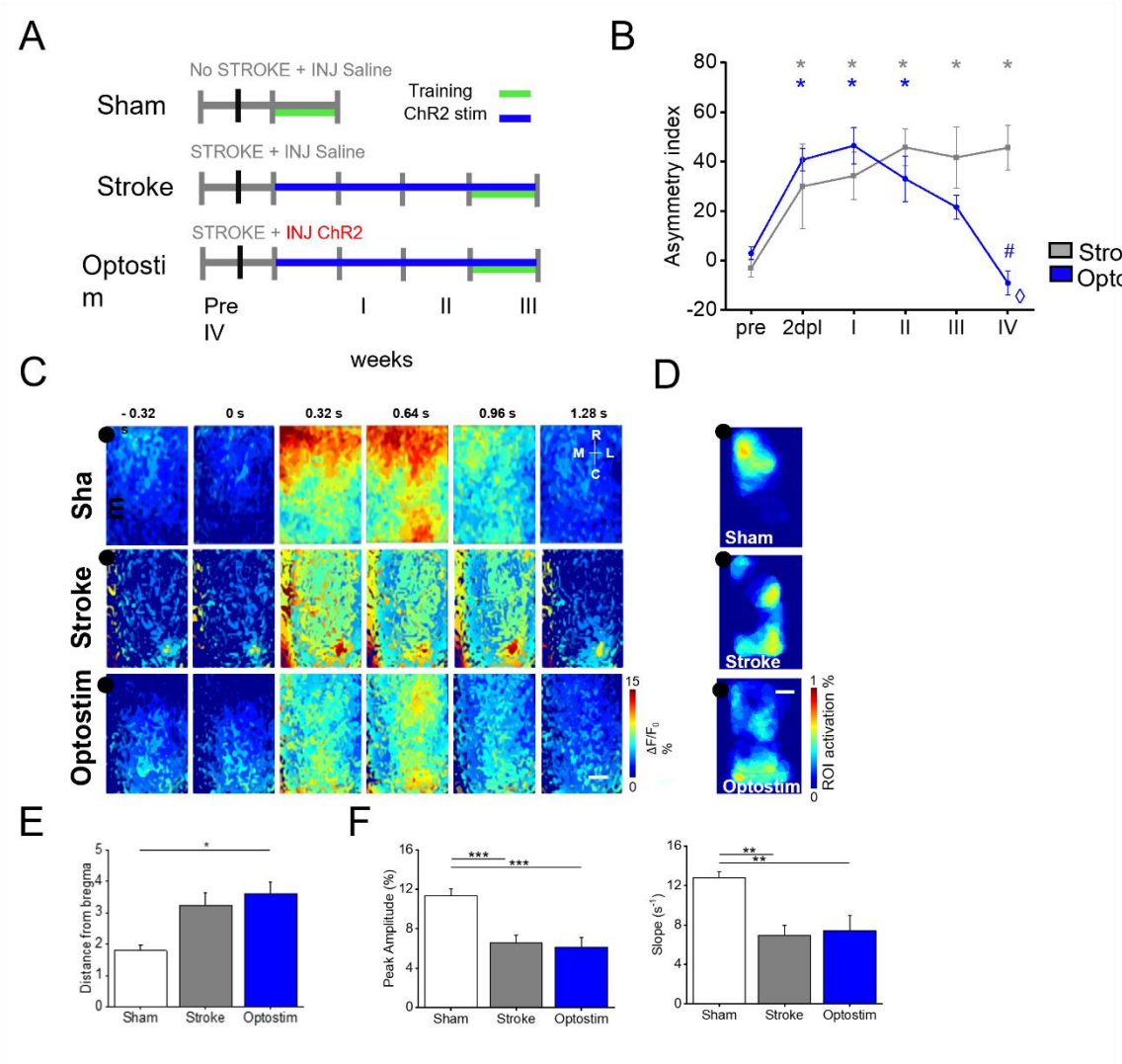

Figure 2. Optogenetic stimulation of peri-infarct area promotes the recovery of forelimb functionality but not the restoration of spatio-temporal cortical profiles: (A) Sham, Stroke and Optostim experimental timeline. (B) Pre- and post-lesion performance of Stroke (Grey) and Optostim (Blue) groups measured as Asymmetry Index in the Schallert cylinder test. *p≤0.05 refers to repeated-measure ANCOVA analysis followed by post-hoc pairwise comparisons for Schallert asymmetry index values of Stroke and Optostim groups pre with respect to the other time points. Stroke group: p pre-2dpl = 0.0012; pre-Iw = 0.0001; pre-IIw < 0.0001; p pre-IIIw< 0.0001; p pre-IVw < 0.0001; Optostim group: p pre-2dpl = 0.0001; p pre-Iw < 0.0001; p pre-IIw=0.005; ◊ p≤0.05 refers to repeated-measure ANCOVA analysis followed by post-hoc pairwise comparisons for Schallert A.i. values of Optostim groups 2dpl with respect to the other

time points 2dpl-IVw<0.0001; p pre-IIw= 0.005. #p≤0.05 refers to repeated-measure ANCOVA analysis followed by post-hoc pairwise comparisons for Schallert A.i. values of Optostim and Stroke groups. Optostim vs Stroke IVw<0.0001 (for statistical pairwise comparison see Supplementary Materials Table 1). (C) Image sequence of cortical activation assessed by calcium imaging during pulling of contralateral forelimb, from 0.32 s before to 1.28 s after the onset of the force peak. Each row shows a representative sequence from a single animal for each group. Scale bar 1mm. (D) Motor-related activation maps show the average thresholded region of maximum activation triggered by the pulling task for each experimental group. Scale bar 1mm. (E) Graph shows the distance from bregma (average ± SEM) of maps centroid (Sham = 1.8 ± 0.2 mm; Stroke = 3.2 ± 0.4 mm; Optostim = 3.6 ± 0.4 mm; *p<0.05 based on one-way ANOVA followed by Tukey's correction: p Sham-Stroke= 0.048; p Sham-Optostim =0.03). (F) Left panel: graph shows the maximum of fluorescence peaks (average ± SEM) of calcium transient (Peak-Amplitude_Sham = 11.3 ± 0.7%; Peak-Amplitude_Stroke = 6.6 ± 0.7%; Peak-Amplitude_Optostim = 6.1 ± 0.9%; ***p<0.0005 based on one-way ANOVA followed by Tukey's correction: p Sham-Stroke= 0.0005; p Sham-Optostim =0.0002). Right panel: graph shows the slope (average ± SEM) of the rising phase of fluorescence traces (Slope_Sham = 12.8 ± 0.6 s^{-1}; Slope_Stroke = 6.9 ± 1.0 s^{-1}, Slope_Optostim = 7.4 ± 1.5 s^{-1}; **p<0.005 based on one-way ANOVA followed by Tukey's correction: p Sham-Stroke = 0.002; p Sham-Optostim = 0.005; for statistical pairwise comparison see Supplementary Materials Table 2). nSham=6; nStroke=4; nOptostim=4.

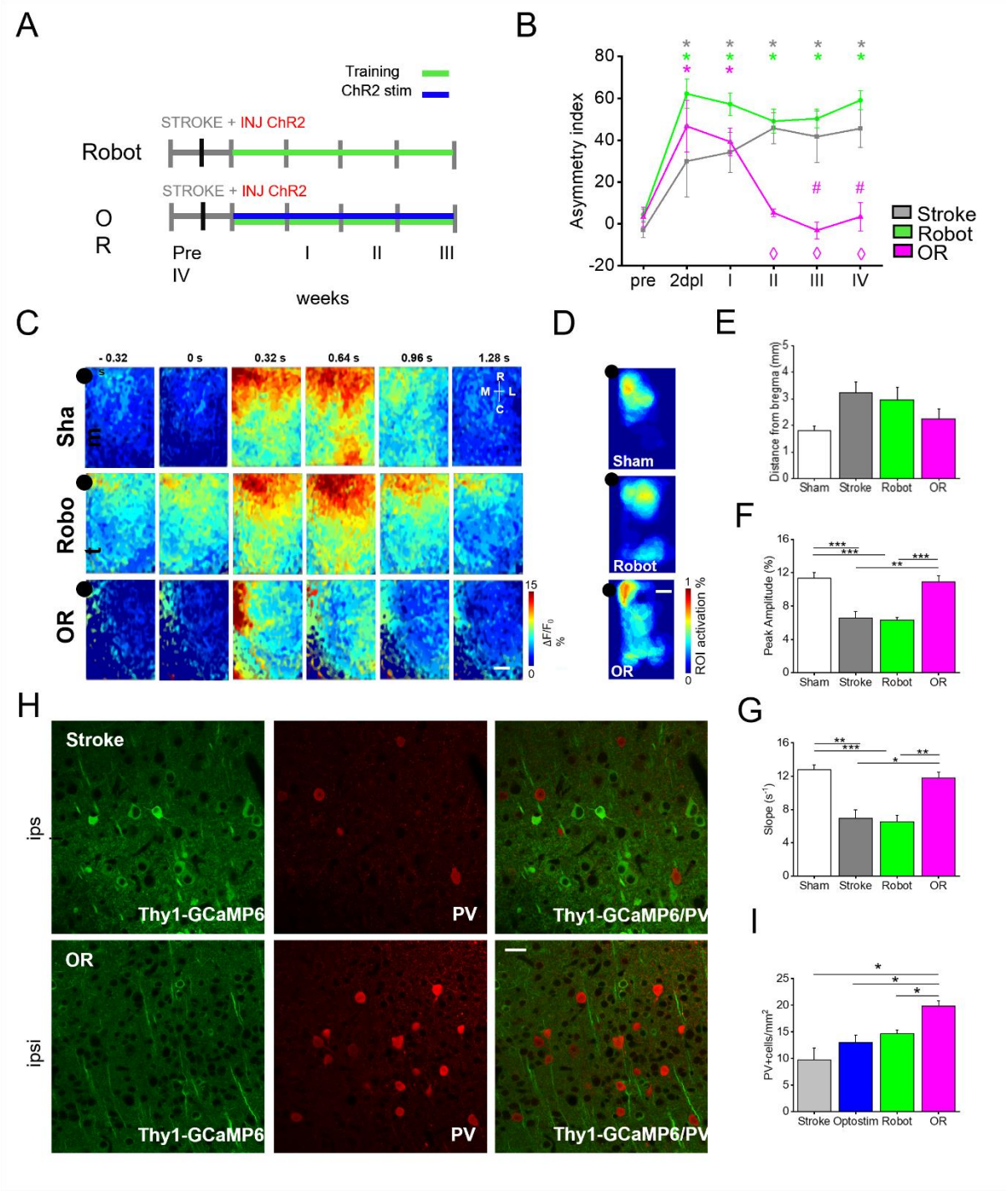

Figure 3. Combining optogenetic stimulation with motor training boosts functional recovery and promotes the restoration of motor-related cortical functionality: (A) Experimental timeline for Robot and OR groups. (B) Pre- and post-lesion performance of Stroke (Grey), Robot (Green), and Optostim+Robot (Magenta) groups measured as Asymmetry Index in the Schallert cylinder test. *p≤0.05 refers to repeated-measure ANCOVA analysis

followed by post-hoc pairwise comparisons for Schallert asymmetry index values of Stroke, Robot and OR groups at different time points. Stroke group: p pre-2dpl = 0.0012; pre-Iw = 0.0001; pre-IIw <0.0001; p pre-IIIw< 0.0001; p pre-IVw <0.0001; Robot group: p pre-2dpl< 0.0001; pre-Iw<0.0001; pre-IIw<0.0001; p pre-IIIw<0.0001; p pre-IVw<0.0001; OR p pre-2dpl<0.0001; pre-Iw<0.0001; ◊ $p \leq 0.05$ refers to repeated-measure ANCOVA analysis followed by post-hoc pairwise comparisons for Schallert A.i. values of OR group 2dpl with respect to the other time points: 2dpl-IIw<0.0001; 2dpl-IIIw<0.0001; 2dpl-IVw<0.0001; #$p \leq 0.05$ refers to repeated-measure ANCOVA analysis followed by post-hoc pairwise comparisons for Schallert asymmetry index values of OR and Stroke groups. OR vs Stroke p wIII=0.02; p wIV=0.05 (for statistical pairwise comparison see Supplementary Materials Table 1). nStroke=4; nRobot=7; nOR=4. (C) Image sequence of cortical activation during pulling of the handle, from 0.32s before to 1.28s after force peak onset. Each row shows a representative sequence from a single animal of each group Sham (repeated from Figure 1), Robot and OR. Scale bar 1mm. Left panel shows the average thresholded ROI computed for each experimental group. Black dot represents bregma. Scale bar 1mm. (E) Graph shows the distance from bregma (average ± SEM) of maps centroid (Sham = 1.8 ± 0.2 mm; Stroke = 3.2 ± 0.4 mm; Robot = 2.9 ± 0.5 mm; OR = 2.2 ± 0.4 mm). (F) The graph shows the maximum of fluorescence peaks (average ± SEM) of calcium transient (Peak-Amplitude_Sham = 11.3 ± 0.7%; Peak-Amplitude_Stroke = 6.6 ± 0.7%; Peak-Amplitude_Robot = 6.3 ± 0.3%; Peak-Amplitude_OR = 10.9 ± 0.7%; *p<0.05, **p<0.005, ***<0.0005 based on one-way ANOVA followed by Tukey's correction: p Sham-Robot = 0.00005; p OR-Stroke= 0.003; p OR- Robot=0.0005). (G) The graph shows the slope (average ± SEM) of the rising phase of fluorescence traces (Slope_Sham = 12.8 ± 0.6 s^{-1}; Slope_Stroke = 6.9 ± 2.0 s^{-1}, Slope_Robot = 6.5 ± 0.8 s^{-1}; Slope_OR = 11.8 ± 0.7 s^{-1}; *p<0.05, **p<0.005, ***<0.0005 based on one-way ANOVA followed by Tukey's correction: pSham-Robot= 0.0002; p OR-Stroke = 0.02; p OR-

Robot=0.004; for statistical pairwise comparison see Supplementary Materials Table 2); (H) Transgenic expression of GCaMP6f under Thy1 promoter (green) and representative PV immunostaining (red) of a Stroke and OR mouse. (I) Quantification of PV+ cells in all groups in the peri-infarct area (Stroke= 9,7 ± 2,2; Optostim= 13,0 ± 1,3; Robot= 14,6 ± 0.7; OR= 19,8 ± 1,0; *p<0.05 based on one-way ANOVA followed by Tukey's correction: p Stroke-OR= 0,0004; p Optostim-OR= 0,006; p Robot-OR= 0,02; for statistical pairwise comparison see Supplementary Materials Table 3). Scale bar 20µm.; nSham=6; nStroke=4; nRobot=7; nOR=4.

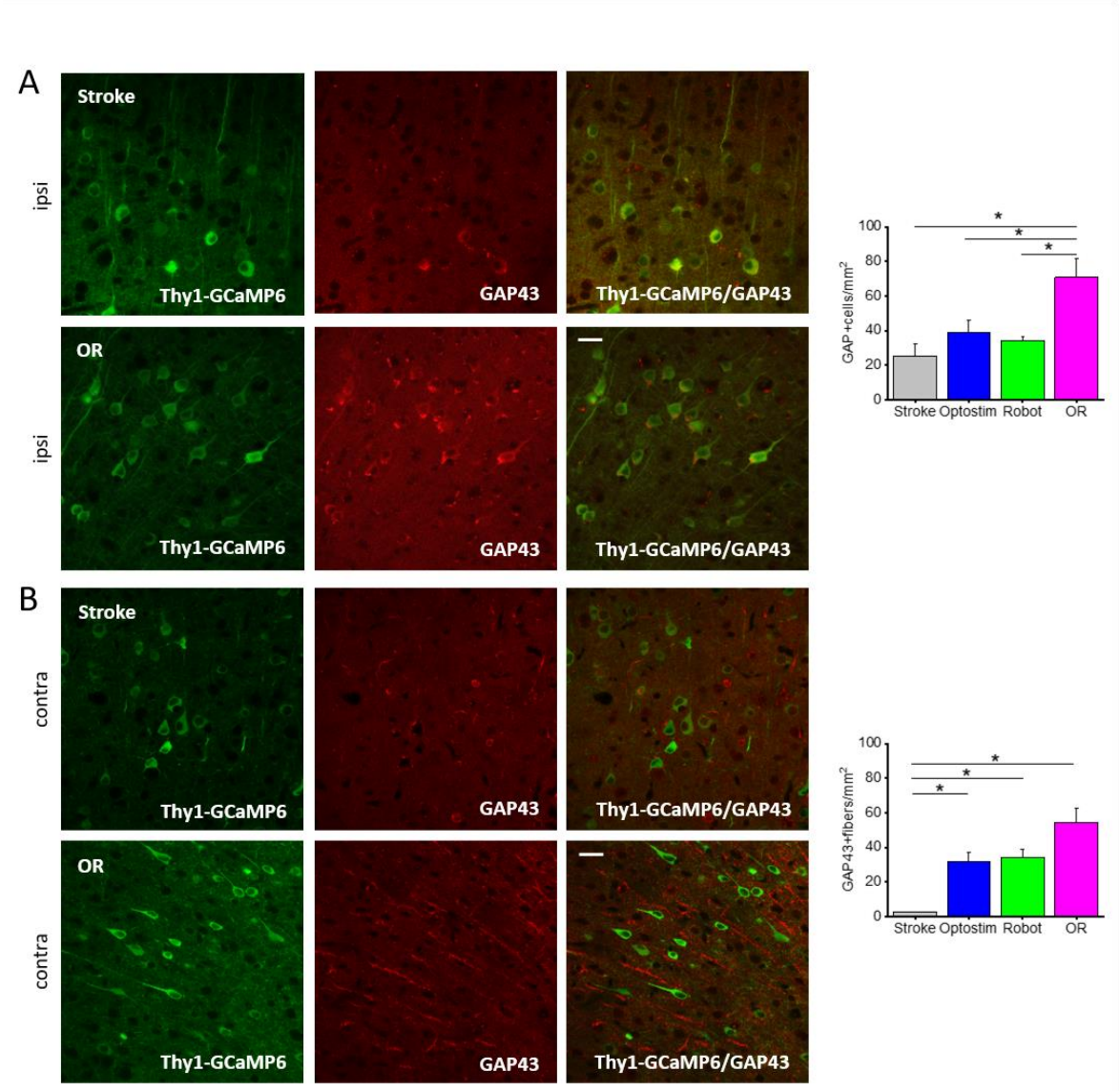

Figure 4. *Ex vivo* evaluation highlights an increased expression of plasticizing factor in OR mice: (A) Left: Transgenic expression of GCaMP6f under Thy1 promoter (green) and

representative GAP43 immunostaining (red) of a coronal section (100µm thick) of a Stroke and OR mouse. Right: quantification of GAP43+ cells in the peri-infarct area in all experimental groups (Stroke= 25,0 ± 7,2; Optostim= 38,7 ± 7,3; Robot= 34,3 ± 2,4; OR= 70,7 ± 10,7; *p<0.05 based on one-way ANOVA followed by Tukey's correction: p Stroke-OR= 0,001; p Optostim-OR= 0,02; p Robot-OR= 0,004). (B) Left: transgenic expression of GCaMP6f under Thy1 promoter (green) and representative GAP43 immunostaining (red) of CL labeled fibers. Right: quantification of GAP43+ fibers in the CL hemisphere (Stroke= 2,4 ± 0,4; Optostim= 31,8 ± 5,4; Robot= 34,0 ± 4,7; OR= 54,4 ± 8,3; *p<0.05 based on one-way ANOVA followed by Tukey's correction: p Stroke-OR= 0,0007; p Optostim-Stroke= 0,04; p Robot-Stroke= 0,01; for statistical pairwise comparison see Supplementary Materials Table 3); Scale bar 20µm; nStroke=4; nOptostim=4; nRobot=7; nOR=4.

References

1. Schwab ME. How hard is the CNS hardware? *Nat Neurosci.* 2010;13(12):1444-1446.
2. Dancause N, Nudo RJ. Shaping plasticity to enhance recovery after injury. *Prog Brain Res.* 2011;192:273-295.
3. Murphy TH, Corbett D. Plasticity during stroke recovery: from synapse to behaviour. *Nat Rev Neurosci.* 2009;10(12):861-872.
4. Zeiler SR, Krakauer JW. The interaction between training and plasticity in the poststroke brain. *Curr Opin Neurol.* 2013;26(6):609-616.
5. Takatsuru Y, Fukumoto D, Yoshitomo M, Nemoto T, Tsukada H, Nabekura J. Neuronal circuit remodeling in the contralateral cortical hemisphere during functional recovery from cerebral infarction. *J Neurosci.* 2009;29(32):10081-10086.
6. Iwai M, Stetler RA, Xing J, et al. Enhanced oligodendrogenesis and recovery of neurological function by erythropoietin after neonatal hypoxic/ischemic brain injury. *Stroke.* 2010;41(5):1032-1037.
7. Zhao Y, Rempe DA. Targeting astrocytes for stroke therapy. *Neurotherapeutics.* 2010;7(4):439-451.
8. Boyden ES, Zhang F, Bamberg E, Nagel G, Deisseroth K. Millisecond-timescale, genetically targeted optical control of neural activity. *Nat Neurosci.* 2005;8(9):1263-1268.
9. Li N, Daie K, Svoboda K, Druckmann S. Robust neuronal dynamics in premotor cortex during motor planning. *Nature.* 2016;532(7600):459-464.
10. Yizhar O, Fenno LE, Davidson TJ, Mogri M, Deisseroth K. Optogenetics in neural systems. *Neuron.* 2011;71(1):9-34.
11. Wahl AS, Buchler U, Brandli A, et al. Optogenetically stimulating intact rat corticospinal tract post-stroke restores motor control through regionalized functional circuit formation. *Nat Commun.* 2017;8(1):1187.

12. Murase N, Duque J, Mazzocchio R, Cohen LG. Influence of interhemispheric interactions on motor function in chronic stroke. *Ann Neurol.* 2004;55(3):400-409.
13. Volz LJ, Vollmer M, Michely J, Fink GR, Rothwell JC, Grefkes C. Time-dependent functional role of the contralesional motor cortex after stroke. *Neuroimage Clin.* 2017;16:165-174.
14. Cheng MY, Wang EH, Woodson WJ, et al. Optogenetic neuronal stimulation promotes functional recovery after stroke. *Proc Natl Acad Sci U S A.* 2014;111(35):12913-12918.
15. Tennant KA, Taylor SL, White ER, Brown CE. Optogenetic rewiring of thalamocortical circuits to restore function in the stroke injured brain. *Nat Commun.* 2017;8:15879.
16. Alia C, Spalletti C, Lai S, et al. Neuroplastic Changes Following Brain Ischemia and their Contribution to Stroke Recovery: Novel Approaches in Neurorehabilitation. *Front Cell Neurosci.* 2017;11:76.
17. Straudi S, Martinuzzi C, Baroni A, et al. Monitoring Step Activity During Task-Oriented Circuit Training in High-Functioning Chronic Stroke Survivors: A Proof-of-Concept Feasibility Study. *Ann Rehabil Med.* 2016;40(6):989-997.
18. Graef P, Dadalt MLR, Rodrigues D, Stein C, Pagnussat AS. Transcranial magnetic stimulation combined with upper-limb training for improving function after stroke: A systematic review and meta-analysis. *J Neurol Sci.* 2016;369:149-158.
19. Hosomi K, Morris S, Sakamoto T, et al. Daily Repetitive Transcranial Magnetic Stimulation for Poststroke Upper Limb Paresis in the Subacute Period. *J Stroke Cerebrovasc Dis.* 2016;25(7):1655-1664.
20. Edwards DJ. On the understanding and development of modern physical neurorehabilitation methods: robotics and non-invasive brain stimulation. *J Neuroeng Rehabil.* 2009;6:3.
21. Edwards DJ, Krebs HI, Rykman A, et al. Raised corticomotor excitability of M1 forearm area following anodal tDCS is sustained during robotic wrist therapy in chronic stroke. *Restor Neurol Neurosci.* 2009;27(3):199-207.
22. Triccas LT, Burridge JH, Hughes A, Verheyden G, Desikan M, Rothwell J. A double-blinded randomised controlled trial exploring the effect of anodal transcranial direct current stimulation and uni-lateral robot therapy for the impaired upper limb in sub-acute and chronic stroke. *NeuroRehabilitation.* 2015;37(2):181-191.
23. Simonetti D, Zollo L, Milighetti S, et al. Literature Review on the Effects of tDCS Coupled with Robotic Therapy in Post Stroke Upper Limb Rehabilitation. *Front Hum Neurosci.* 2017;11:268.
24. Dana H, Chen TW, Hu A, et al. Thy1-GCaMP6 transgenic mice for neuronal population imaging in vivo. *PLoS One.* 2014;9(9):e108697.
25. Pasquini M, Lai S, Spalletti C, et al. A Robotic System for Adaptive Training and Function Assessment of Forelimb Retraction in Mice. *IEEE Trans Neural Syst Rehabil Eng.* 2018;26(9):1803-1812.
26. Spalletti C, Lai S, Mainardi M, et al. A robotic system for quantitative assessment and poststroke training of forelimb retraction in mice. *Neurorehabil Neural Repair.* 2014;28(2):188-196.
27. Conti E, Allegra Mascaro AL, Pavone FS. Large Scale Double-Path Illumination System with Split Field of View for the All-Optical Study of Inter-and Intra-Hemispheric Functional Connectivity on Mice. *Methods Protoc.* 2019;2(1).
28. Crocini C, Ferrantini C, Coppini R, et al. Optogenetics design of mechanistically-based stimulation patterns for cardiac defibrillation. *Sci Rep.* 2016;6:35628.
29. Turrini L, Fornetto C, Marchetto G, et al. Optical mapping of neuronal activity during seizures in zebrafish. *Sci Rep.* 2017;7(1):3025.
30. Cecchini G, Scaglione A, Allegra Mascaro AL, et al. Cortical propagation tracks functional recovery after stroke. *PLoS Comput Biol.* 2021;17(5):e1008963.
31. Allegra Mascaro AL, Conti E, Lai S, et al. Combined Rehabilitation Promotes the Recovery of Structural and Functional Features of Healthy Neuronal Networks after Stroke. *Cell Rep.* 2019;28(13):3474-3485 e3476.

32. Spalletti C, Alia C, Lai S, et al. Combining robotic training and inactivation of the healthy hemisphere restores pre-stroke motor patterns in mice. *Elife.* 2017;6.
33. Paxinos G, Franklin KBJ. The Mouse Brain in Stereotaxic Coordinates. 1997.
34. Carmichael ST, Archibeque I, Luke L, Nolan T, Momiy J, Li S. Growth-associated gene expression after stroke: evidence for a growth-promoting region in peri-infarct cortex. *Exp Neurol.* 2005;193(2):291-311.
35. Carmichael ST. Plasticity of cortical projections after stroke. *Neuroscientist.* 2003;9(1):64-75.
36. Carmichael ST. Cellular and molecular mechanisms of neural repair after stroke: making waves. *Ann Neurol.* 2006;59(5):735-742.
37. Li S, Carmichael ST. Growth-associated gene and protein expression in the region of axonal sprouting in the aged brain after stroke. *Neurobiol Dis.* 2006;23(2):362-373.
38. Schaden H, Stuermer CA, Bahr M. GAP-43 immunoreactivity and axon regeneration in retinal ganglion cells of the rat. *J Neurobiol.* 1994;25(12):1570-1578.
39. Benowitz LI, Routtenberg A. GAP-43: an intrinsic determinant of neuronal development and plasticity. *Trends Neurosci.* 1997;20(2):84-91.
40. DiFiglia M, Roberts RC, Benowitz LI. Immunoreactive GAP-43 in the neuropil of adult rat neostriatum: localization in unmyelinated fibers, axon terminals, and dendritic spines. *J Comp Neurol.* 1990;302(4):992-1001.
41. Sakadzic S, Lee J, Boas DA, Ayata C. High-resolution in vivo optical imaging of stroke injury and repair. *Brain Res.* 2015;1623:174-192.
42. Cheng MY, Aswendt M, Steinberg GK. Optogenetic Approaches to Target Specific Neural Circuits in Post-stroke Recovery. *Neurotherapeutics.* 2016;13(2):325-340.
43. Montagni E, Resta F, Mascaro ALA, Pavone FS. Optogenetics in Brain Research: From a Strategy to Investigate Physiological Function to a Therapeutic Tool. *Photonics.* 2019;6(3):92.
44. Pendharkar AV, Levy SL, Ho AL, Sussman ES, Cheng MY, Steinberg GK. Optogenetic modulation in stroke recovery. *Neurosurg Focus.* 2016;40(5):E6.
45. Bauer AQ, Kraft AW, Wright PW, Snyder AZ, Lee JM, Culver JP. Optical imaging of disrupted functional connectivity following ischemic stroke in mice. *Neuroimage.* 2014;99:388-401.
46. Song M, Yu SP, Mohamad O, et al. Optogenetic stimulation of glutamatergic neuronal activity in the striatum enhances neurogenesis in the subventricular zone of normal and stroke mice. *Neurobiol Dis.* 2017;98:9-24.
47. Butefisch CM. Neurobiological bases of rehabilitation. *Neurol Sci.* 2006;27 Suppl 1:S18-23.
48. Jinno S, Kosaka T. Parvalbumin is expressed in glutamatergic and GABAergic corticostriatal pathway in mice. *J Comp Neurol.* 2004;477(2):188-201.
49. Lee AT, Vogt D, Rubenstein JL, Sohal VS. A class of GABAergic neurons in the prefrontal cortex sends long-range projections to the nucleus accumbens and elicits acute avoidance behavior. *J Neurosci.* 2014;34(35):11519-11525.
50. Rock C, Zurita H, Lebby S, Wilson CJ, Apicella AJ. Cortical Circuits of Callosal GABAergic Neurons. *Cereb Cortex.* 2018;28(4):1154-1167.
51. Swanson OK, Maffei A. From Hiring to Firing: Activation of Inhibitory Neurons and Their Recruitment in Behavior. *Front Mol Neurosci.* 2019;12:168.

Supplementary Materials

Mice

All procedures involving mice were performed in accordance with the regulations of the Italian Ministry of Health authorization n. 871/2018. Mice were housed in clear plastic cages under a 12 h light/dark cycle and were given ad libitum access to water and food. We used a transgenic mouse line, C57BL/6J-Tg(Thy1GCaMP6f)GP5.17Dkim/J, from Jackson Laboratories (Bar Harbor, Maine USA). This transgenic mouse line expresses the green fluorescent indicator in a subset of excitatory neurons, i.e. pyramidal neurons[24]. To compute the number of subjects per group we conducted a power analysis considering a one way ANOVA (fixed effects, omnibus, one-way) with an effect size f = 1.0, $\alpha = 0.05$ and Power = 0.8 (software used G * Power, version 3.1.9.2, Franz Faul, University of Kiel, Germany). We estimated the minimum number of animals required to measure an improvement in the motor outcomes, based on the results of our previous paper (Allegra and Conti et al. 2019)[31]. From data presented in Figure 3 of Allegra and Conti et al. (2019), we estimated an effect size of 1.0 that was used to calculate the minimum number of animals necessary for this study to obtain a power = 80. The software calculated that the number of 4 animals per group was enough to have a power of ≈ 80. Mice were identified by earmarks and numbered accordingly. Animals were randomly divided into 5 groups and distributed as follows: Sham n=6; Stroke n=4; Optostim n=4; Robot= 7; Optostim+Robot (abbreviated in OR) n= 4. Each group contained comparable numbers of male and female mice (weighing approximately 25g). The age of mice (ranging from 6 to 8 months old) was consistent between the groups.

Channelrhodopsin-2 (ChR2) injection

All surgical procedures were performed under isoflurane anesthesia (3% induction, 1.5% maintenance, in 1L/min oxygen). Body temperature was maintained at 37°C and mice were monitored using respiratory rate and toe pinch throughout the procedure. The animals were

placed into a stereotaxic apparatus (Stoelting, Wheat Lane, Wood Dale, IL 60191). The skin over the skull was cut and the periosteum was removed with a blade. We used a dental drill to create a small craniotomy over somatosensory cortex, which was identified by stereotaxic coordinates. We injected 0.5 μL of AAV9-CaMKIIa-hChR2(H134R)-mCherry (2.48*1013 GC/mL) 600 μm deep inside the cortex at (i) -0.75 anteroposterior, +1.75 mediolateral.

We longitudinally evaluated ChR2 expression along the weeks starting 5 days after the intracortical injection. As shown in the Supplementary Figure 1 C and D, ChR2 expression was assessed *in vivo* by acquiring through-skull fluorescence images of the reporter mCherry, which was co-transfected by our viral vector AAV9-CaMKIIa-hChR2(H134R)-mCherry. mCherry fluorescence was revealed on a wide fluorescent region of the cortex around the injection site from the first imaging session (day 5 post injection) in all transfected mice (the black spot on the top left corner of the image labels bregma). At the end of the rehabilitative period, 30 days after the injection, ChR2 expression is evenly distributed across the cortex layers and it extends for 600 μm in the rostro-caudal direction.

In Stroke, Optostim, Robot and OR mice this surgery was followed by the stroke induction. Robot mice were injected with ChR2 though the animals will not be optogenetically stimulated. We applied this precaution not to underestimate a possible effect of LED excitation of ChR2 expressing neurons during calcium imaging. In Sham mice a cover glass and an aluminum head-post were attached to the skull using transparent dental cement (Super Bond, C&S), then the animals were placed in a heated cage (temperature 38°) until they fully recovered. Given the design of the experiment, no blind approach was applied during surgery. Channel rhodopsin injections were performed during the same surgical session in which the photothrombotic lesions were generated.

Photothrombotic lesion

The primary motor cortex (M1) was identified (stereotaxic coordinates +1,75 lateral, +0.5 rostral from bregma). Five minutes after intraperitoneal injection of Rose Bengal (0.2 ml, 10 mg/ml solution in Phosphate Buffer Saline (PBS); Sigma Aldrich, St. Louis, Missouri, USA), white light from an LED lamp (CL 6000 LED, Carl Zeiss Microscopy, Oberkochen, Germany) was focused with a 20X objective (EC Plan Neofluar NA 0.5, Carl Zeiss Microscopy, Oberkochen, Germany) and used to illuminate the M1 for 15 min to induce unilateral stroke in the right hemisphere. Sham mice were injected with 0.2 mL of saline and then illuminate as the others. A cover glass and an aluminum head-post were attached to the skull using transparent dental cement (Super Bond, C&S). We waited at least 4-5 days after the surgery for the mice to recover before the first imaging session. After the last imaging session, all animals were perfused first with 20-30 mL of 0.01 M PBS (pH 7.6) and then with 150 mL of Paraformaldehyde 4% (PFA, Aldrich, St. Louis, Missouri, USA).

Robotic rehabilitation

Mice were allowed to become accustomed to the apparatus before the first imaging session so that they became acquainted with the new environment. The animals were trained by means of the M-Platform[26], which is a robotic system that allows mice to perform a retraction movement of their left forelimb . Briefly, the M-Platform is composed of a linear actuator, a 6-axis load cell, a precision linear slide with an adjustable friction system and a custom-designed handle that is fastened to the left wrist of the mouse. The handle is screwed onto the load cell, which permits a complete transfer of the forces applied by the animal to the sensor during the training session. Each training session was divided into “trials” that were repeated sequentially and consisted of 5 consecutive steps. First, the linear actuator moved the handle forward and extended the mouse left forelimb by 10 mm (full upper extremity extension). Next, the actuator quickly decoupled from the slide and a tone lasting 0.5 s informed the mouse that it should initiate the task. If the animal was able to overcome the static friction (approximately 0.2 N), it

voluntarily pulled the handle back by retracting its forelimb (i.e. forelimb flexion back to the starting position). Upon successful completion of the task, a second tone that lasted 1 sec was emitted and the animal was given access to a liquid reward, i.e. 10 µl of sweetened condensed milk, before starting a new cycle. To detect the movement of the wrist of the animal in the low-light condition of the experiment, an infrared (IR) emitter was placed on the linear slide, and rigidly connected to the load cell and thus to the animal's wrist. Slide displacement was recorded by an IR camera (EXIS WEBCAM #17003, Trust) that was placed perpendicular to the antero-posterior axis of the movement. Position and speed signals were subsequently extracted from the video recordings and synchronized with the force signals recorded by the load cell (sampling frequency = 100 Hz). To adjust the friction of the device, a calibration procedure was performed by connecting the actuator with the slide using a rigid component. This component mimics the effect of the retraction movements performed by the animal, reproducing the applied forces in direction and point of application. The training consisted of 15 cycles of passive extension of the affected forelimb followed by its active retraction triggered by the acoustic cue. All groups performed at least one week (5 sessions) of daily training, starting 26 days after injury for Stroke and Optostim mice, 5 days after stroke for Robot and OR groups and after the surgery for Sham animals. During the last week of optogenetic stimulation of Optostim and Stroke mice and the entire rehabilitative period for OR mice the robotic training is followed by the optogenetic stimulation.

Optogenetic stimulation

Awake head-fixed mice were placed under the wide-field microscope to perform daily session of optogenetic stimulation. A blue 473 nm laser is used to deliver 5 Hz, 10ms light pulses similar to Tennant 2017[15]. The laser power used, ranging from 0.2 to 0.8 mW, was lower than the one necessary to elicit movements of the affected forelimb during cortical optogenetic stimulation. Furthermore, the laser power is adjusted during the rehabilitation period, to provide

a reproducible stimulation according to the increment of the transfected area and the progressive lowering of stimulation threshold over the weeks. The system is provided with a random-access scanning head, developed using two orthogonally mounted acousto-optical deflectors (DTSXY400, AA Opto-Electronic). The acousto-optic deflectors rapidly scan lines with a commutation time ~5 μs between a line and the next. After scanning the desired shape (in this case a cross) in the area of the cortex of ChR2 maximum expression (approximately near the injection site -0.75 anteroposterior, +1.75 mediolateral), the acousto-optic deflectors returned to the initial position and repeated the cycle for the total illumination time. The stimulation protocol consists of 3 successive 30 s stimulation daily separated by 1 min rest intervals. All animals (Stroke, Optostim and OR), except for Sham and Robot groups, were stimulated every day for 4 weeks, 5 days after photothrombosis. Optostim and OR groups are exposed to optogenetic stimulation approximately 5 minutes after the execution of the last pulling during motor rehabilitation. We stimulated Stroke mice not expressing ChR2 to evaluate possible artefacts due to repeated laser stimulation. All the experiments revealed that repeated stimulation of mouse cortex not expressing ChR2 did not affect post-stroke recovery.

Schallert Cylinder Test

Mice were placed in a Plexiglas cylinder (7,5 cm diameter, 16 cm height) and recorded for five minutes by a webcam placed below the cylinder, after 2 minutes of acclimatization. Videos were analyzed frame by frame and the spontaneous use of both forelimbs was assessed during exploration of the walls, by counting the number of contacts performed by the paws of the animal. For each wall exploration, the last paw that left and the first paw that contacted the wall or the ground were assessed. The analysis was conducted in blind. In order to quantify forelimb-use asymmetry displayed by the animal, an Asymmetry index was computed, according to Lai et al. 2015[52] with the following formula : $\mathrm{Ai} = \left(\frac{C_{ipsi}}{C_{ipsi}+C_{contra}}\right) \times 100 - \left(\frac{C_{contra}}{C_{ipsi}+C_{contra}}\right) \times 100.$

Wide-field fluorescence microscope

The custom-made wide-field imaging setup was equipped with two excitation sources allowing imaging of GCaMP6f fluorescence and light-stimulation of ChR2. For imaging of GCaMP6f fluorescence, a 505 nm LED (M505L3 Thorlabs, New Jersey, United States) light was deflected by a dichroic filter (DC FF 495-DI02 Semrock, Rochester, New York USA) on the objective (2.5x EC Plan Neofluar, NA 0.085, Carl Zeiss Microscopy, Oberkochen, Germany). A 3D motorized platform (M-229 for xy plane, M-126 for z-axis movement; Physik Instrumente, Karlsruhe, Germany) allowed sample displacement. The fluorescence signal was selected by a band-pass filter (525/50 Semrock, Rochester, New York USA). Then a 20X objective (LD Plan Neofluar, 20x/0.4 M27, Carl Zeiss Microscopy, Oberkochen, Germany) was used to demagnify the image onto a 100X100 pxl^2 area of the sCMOS camera sensor (OrcaFLASH 4.0, Hamamatsu Photonics, NJ, USA). Images (5.2 x 5.2 mm^2, pixel size 52 µm) were acquired at 25 Hz. To perform optogenetic stimulation of ChR2, a 473 nm continuous wavelength (CW) laser (OBIS 473nm LX 75mW, Coherent, Santa Clara, California, United States) was overlaid on the imaging path using a second dichroic beam splitter (FF484-Fdi01-25x36, Semrock, Rochester, New York USA) and scanned with two orthogonally-mounted acousto-optical deflectors as previously described (DTSXY400, AA Opto-Electronic, Orsay France).

Image analysis

Analysis of the fluorescence image stacks were previously reported in Allegra et al. 2019[31]. We aimed to characterize activation maps and calcium transient critical features, focusing those transients occurring in the time-window of retraction movement. For each stack we first computed the median time series of GCaMP6f fluorescence signal by computing the median value of fluorescence over all the pixels for each frame of the given stack. The median time series was then oversampled and synchronized to the 100 Hz force and position signals. This time series was used to define a GCaMP6f fluorescence signal baseline F_0, which was identified by the concomitant absence of fluorescence and force signal deflections. F_0 was selected within

a 2.5 ± 0.7 s interval of 62 frames where the fluorescence signal was below 1 standard deviation of the whole recorded force signal. The onset of each force peak was used as a reference time point to select a sequence of 60 frames (2.4 s, where 0.4 s preceded the force peak) for each image stack. All sequences were visually checked to exclude from the analysis spurious activation, such as early activation or no activation, i.e. sequences where the calcium activity in the 8 frames before the onset of the force peak was as high as in the post pull window or sequences where calcium activity did not change after the onset of the force peak, respectively. For each day, all activation sequences were concatenated and used to compute a selected Summed Intensity Projection (SIP) for the animal for that day. The most active area of the SIP was then detected by picking pixels whose values were higher than the median of the SIP plus one standard deviation of the SIP. The threshold SIP was computed for each day of each week of training on the M-Platform (d = 1,.,4 of a given week) the SIPs for each day were superimposed and the common areas, activated at least for 3 daily sessions out of 5 (60%), were selected as Region of Interest (ROI) for the week.

We also used the ROIs defined for each individual animal to identify the average ROIs among mice from the same experimental group (Figure 2D, 3D). The ROIs defined for each individual animal were further used to extract the GCaMP6f fluorescence signal corresponding to the activity of those areas. Indeed, from each frame of the fluorescence stack, only pixels belonging to the selected ROI were considered when calculating the representative median value. Thus, a median time series was extracted from the whole fluorescence stack only in the ROI. The fluorescence signal in the ROI was normalized by computing the $\Delta F/F_0$ (%) and low-pass filtered to clean the signal from the detected heart-beat artifacts (Chebyshev filter with cutting frequency = 9 Hz). The previously detected force peaks were then used to select the GCaMP6f fluorescence peaks from the $\Delta F/F_0$ signal. A time window that lasted 4 s, and was centered at the onset of the force peak, was used to identify the corresponding fluorescence peak. Finally,

a fluorescence peak was defined as the value of $\Delta F/F_0$ that passed the value of median +3 standard deviations of the whole $\Delta F/F_0$.

Force analysis

To quantify the behavior of each animal on the platform we analyzed the force exerted by the mouse during the retraction phase. For each peak associated with the slide movement we extracted 4 parameters: 1) peak amplitude as its max value; 2) peak width (full width at half maximum) as the width of the peak at half the peak amplitude as indirect measure of the power applied by the affected forelimb on the handle; 3) peak area as area of the force signal during its peak width and 4) the time to target as the time between the start of the trial and the peak associated with the last movement of the slide in the trial.

Immunohistochemical analysis

For immunohistochemical analysis of plasticity markers, animals were transcardially perfused with 4% paraformaldehyde. Brains were cut using a vibrating-blade vibratome (Leica, Germany) to obtain 100 µm thick coronal sections that were used for immunostaining of NeuN (1:200, Millipore, Germany), Parvalbumin (1:500, Abcam, United Kingdom) and GAP 43 (1:600, Abcam, United Kingdom). The number of Parvalbumin- and GAP43- positive neurons was analyzed using a confocal fluorescence microscope (Nikon Eclipse TE 300, Tokyo, Japan) with a Nikon Plan EPO 60× objective (NA 1.4, oil immersion Nikon, Tokyo, Japan), acquiring 212 µm wide images in the peri-infarct cortex (up to 600 µm from the damage in the caudal direction). For GAP43 and PV evaluations three sections per animal were analyzed. In each section the 3 images (212x212 µm ^{2}) including layer II/III and V of the cortex (from the longitudinal fissure up to 2 mm in the mediolateral direction) were acquired. We excluded the corpus callosum from the quantification of the fibers. The single fibers revealed in the contralesional hemisphere were measured in the same brain section used for the ipsilesional oneTo evaluate the extension of the lesion we use a 10× objective (C-Apochromat, 0.45 NA,

Carl Zeiss Microscopy, Oberkochen, Germany field of view 1.3 mm). Then, the stroke volume for each animal was calculated by summing up all damaged areas and multiplying the number by section thickness and by 3 (the spacing factor). A total volume in mm^3 is given as the mean ± standard error of all analyzed animals (n=15). The experimenter was blind to the experimental group of the samples.

Reagent identification

REAGENT or RESOURCE	SOURCE	IDENTIFIER
Antibodies		
NeuN	Merck	ABN78
GAP43	Abcam	Ab16053
PV	Abcam	Ab11427
Alexa Fluor 568 Goat anti Rabbit	Abcam	Ab175471
Virus Strains		
AAV9-CaMKII-ChR2-mCherry	DBA Italia	VB4411
Chemicals, Peptides, and Recombinant Proteins		
Zoletil	Virbac	101580025
Xylazine	Dechra	103595017
Rose Bengal	Sigma	330000
Phosphate Buffer Saline	Sigma	P-4417
Lidocaine 2%	Zoetis Italia srl	100319019
Dexamethasone	MSD	101866034
Paraformaldehyde	Sigma	158127
Experimental Models: Organisms/Strains		
Mouse: C57BL/6J-Tg(Thy1GCaMP6f)GP5	The Jackson Laboratories	025393

Software and Algorithms		
ImageJ	Schneider et al., 2012	https://imagej.nih.gov/ij/

Supplemental Figures and Tables

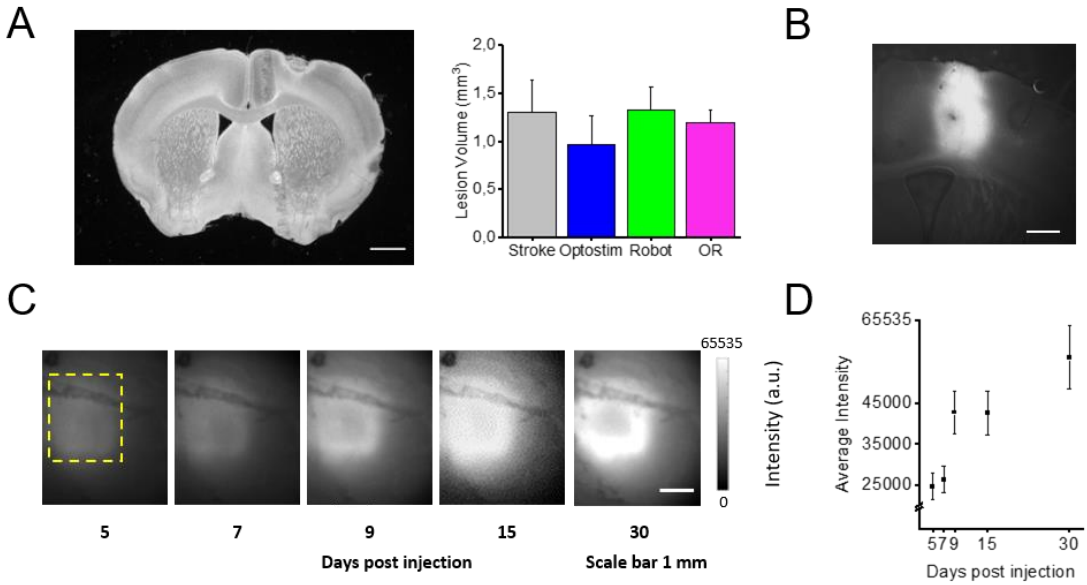

Supplementary Figure 1. (A) Coronal section of a mouse brain 30 days after photothrombosis, 1 mm scale bar. The right panel shows the quantification of the lesioned area in the experimental groups (average ± SEM): Stroke=1,31 ± 0,32 mm^2; Optostim=0,96 ± 0,3 mm^2; Robot=1,33 ± 0,24 mm^2; OR=1,2 ± 0,13 mm^2. (B) Coronal section of a mouse brain transfected with ChR2 30 days after the injection, 0.5 mm scale bar. (C) Longitudinal imaging of mCherry fluorescence to evaluate ChR2 expression in the peri-infarct area during the first week of stimulation (starting 5 days after the injection) (D) Quantification of average intensity (Average ± SD) of mCherry fluorescence during the first week of stimulation (d5 = 24645.0 ± 3163.8; d7 = 24594.2 ± 3216.3; d9 =42896.1 ± 5171.7; d15 = 42723.5 ± 5332.1; d30 = 56383.1 ± 7774.3).

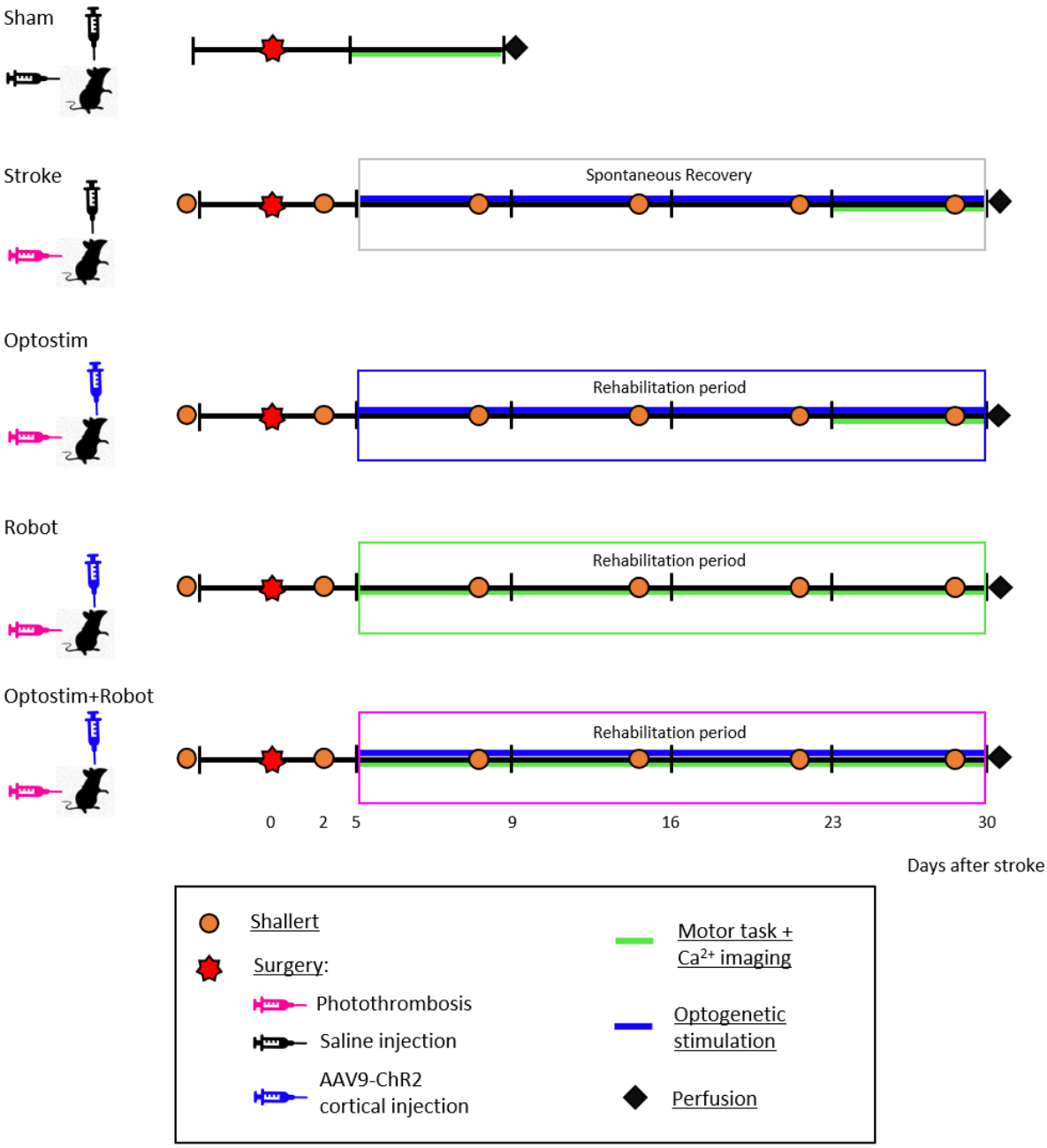

Supplementary Figure 2. Schematic of the treatment protocols. Baseline performances in behavioral tests (orange dot) were assessed for all groups before the surgery and then once a week up to 30 days after the lesion. The last day of treatment mice were perfused (black rhombus).

Sham: ip injection of saline (no stroke), intra cortical injection of saline (no ChR2 expression). 5 days of motor assessment on the M-Platform.

Stroke: stroke, ip injection of Rosebengal, intra cortical injection of saline (no ChR2 expression). 4 weeks of peri-infarct laser stimulation. 5 days of motor assessment on the M-Platform, 26 days after the lesion.

Optostim: stroke, ip injection of Rosebengal, intra cortical injection of AAV9 (ChR2 expression). 4 weeks of peri-infarct laser stimulation. 5 days of motor assessment on the M-Platform, 26 days after the lesion.

Robot: stroke, ip injection of Rosebengal, intra cortical injection of AAV9 (ChR2 expression, no laser stimulation). 4 weeks of motor rehabilitation on the M-Platform, starting 5 days after the lesion.

Optostim+Robot (OR): stroke, ip injection of Rosebengal, intra cortical injection of AAV9 (ChR2 expression). 4 weeks of motor rehabilitation on the M-Platform and laser stimulation, starting 5 days after the lesion.

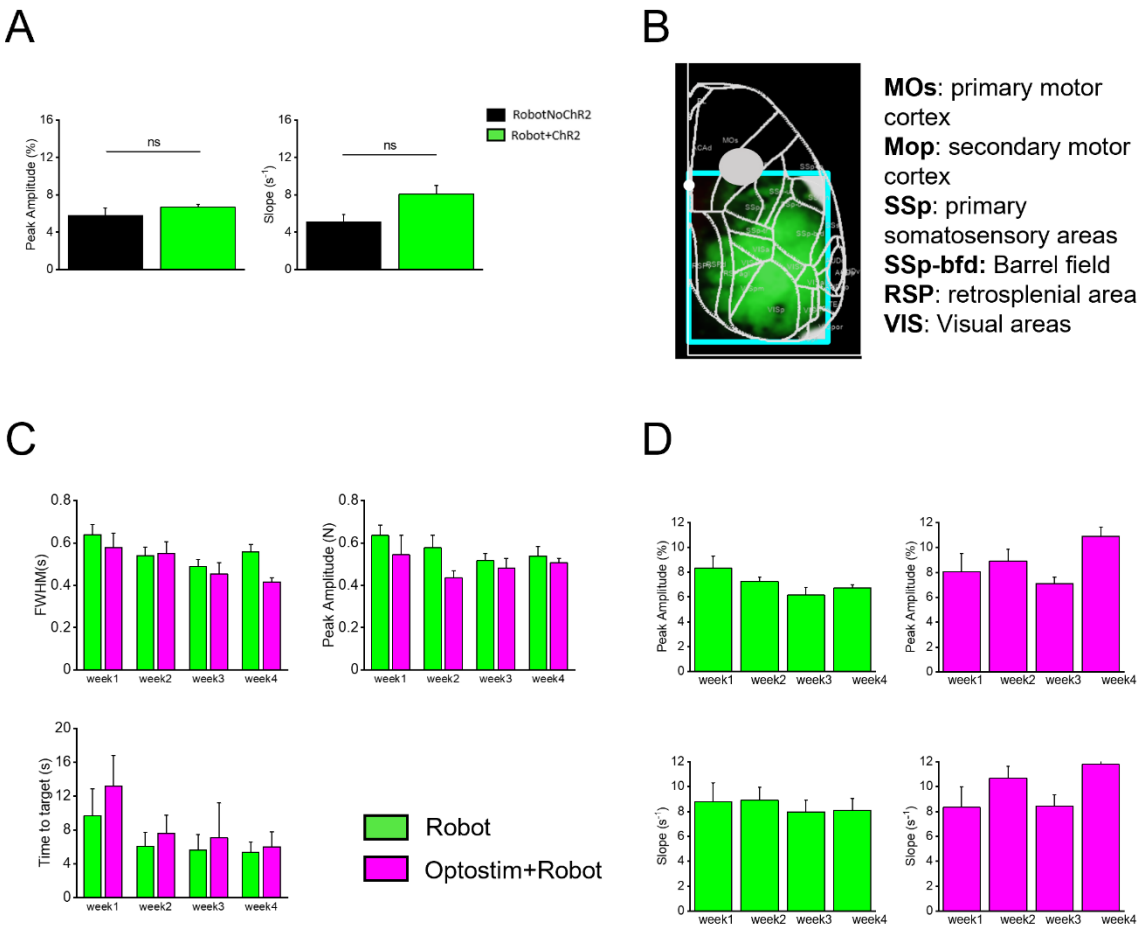

Supplementary Figure 3. (A) The graphs show calcium transient analysis for Robot mice expressing ChR2 (n=5) in the peri-infarct cortex or not (n=3). The left panel shows the Peak Amplitude (average ± SEM) Robot+ChR2 = 6.7 ± 0.3%; RobotNoChR2 = 5.8 ± 0.8%. The right panel shows the Slope (average ± SEM) Robot+ChR2= 8.1 ± 0.9 s^{-1}; RobotNoChR2= 5.1 ± 0.8 s^{-1}. (B) Graphical representation of functional regions of the cortex acquired in the imaging area (cyan square) including primary and secondary motor area, primary somatosensory and barrel field, retrosplenial and primary visual areas. The gray circle on the M1 region highlights the location and approximate extent of the lesion. White dot indicates bregma. (C) Force analysis during pulling task (average ± SEM). Left upper panel shows the Full Width Half Maximum of the force peak (Robot_Iw= 0,64 ± 0,05; OR_Iw= 0,58 ± 0,07; Robot_IIw= 0,54 ± 0,04; OR_IIw= 0,55 ± 0,06; Robot_IIIw= 0,49 ± 0,03; OR_IIIw= 0,45 ± 0,05; Robot_IVw= 0,56 ± 0,04; OR_IVw= 0,42 ± 0,02). Right upper panel show the Peak Amplitude (Robot_Iw= 0,63 ± 0,05; OR_Iw= 0,54 ± 0,18; Robot_IIw= 0,58 ± 0,06; OR_IIw= 0,43 ± 0,06; Robot_IIIw= 0,52 ± 0,03; OR_IIIw= 0,48 ± 0,04; Robot_IVw= 0,54 ± 0,04; OR_IVw= 0,5 ± 0,04) and the lower panel shows the Time to Target (Robot_Iw= 9,7 ± 3,2; OR_Iw= 13,2 ± 3,6; Robot_IIw= 6,1 ± 1,6; OR_IIw= 7,6 ± 2,1; Robot_IIIw= 5,6 ± 1,8; OR_IIIw= 7,1 ± 4,1; Robot_IVw= 5,4 ± 1,2; OR_IVw= 6,0± 1,8). (D) Longitudinal analysis of cortical activation profiles over the 4 weeks for Robot (Amplitude: Iw= 8.3 ± 1.0; IIw= 7.3± 0.3; III= 6.1± 0.6; IV= 6.7 ±0.3; Slope: Iw= 8.8± 1.5; IIw= 8.9 ± 1.0; III= 8.0 ± 0.9; IV= 8.1 ± 0.9) and OR groups (Amplitude: Iw=8.1 ± 1,4; IIw= 8.9 ± 0.9; III= 7.1 ± 0.5; IV= 10.9 ± 0.7; Slope: Iw= 8.3 ± 1.6; IIw= 10.7 ± 0.9; III= 8.4 ± 0.9; IV= 11,8 ± 0.7) same groups legend as in panel C.

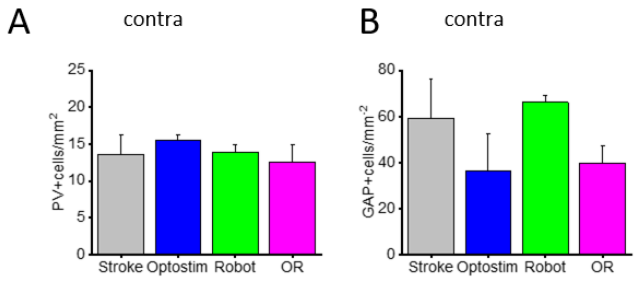

Supplementary Figure 4. (A) Quantification of PV+ cells in the contralesional hemisphere (Stroke= 13,6 ± 2,6; Optostim= 15,5 ±0, 7; Robot= 13,8 ± 1,1; OR= 12,2 ± 3,3). (B) Quantification of GAP43+ cells in the contralesional hemisphere (Stroke= 59,1 ± 16,9; Optostim= 36,5 ± 16,1; Robot= 65,3 ± 1,2; OR=39,6 ± 7,6).

	p (Tukey) A.i. pre	p (Tukey) A.i. 2dpl	p (Tukey) A.i. I week	p (Tukey) A.i. II week	p (Tukey) A.i. III week	p (Tukey) A.i. IV week
Optostim-Stroke	1	1	1	0.5527	0.1266	<0.0001
Robot-Stroke	1	0.3239	0.9506	0.9998	1	1
Robot-Optostim	1	0.44	0.9973	0.8763	0.0644	<0.0001
OR-Stroke	1	0.2056	0.9289	0.0797	0.0228	0.0496
OR-Optostim	1	0.4646	0.9971	0.9993	1	0.1412
OR-Robot	1	1	1	0.4023	0.0484	0.0258

	Stroke	Optostim	Robot	OR
Pre-2dpl	0.0012	0.0001	<0.0001	<0.0001
Pre-Iweek	0.0001	<0.0001	<0.0001	<0.0001
Pre-IIweek	<0.0001	0.0047	<0.0001	0.6602
Pre-IIIweek	<0.0001	0.3523	<0.0001	0.9994
Pre-IVweek	<0.0001	0.9203	<0.0001	0.8278
2dpl-Iweek	1	0.9999	0.997	0.9989
2dpl-IIweek	0.6274	0.9984	0.4721	<0.0001
2dpl-IIIweek	0.9324	0.3113	0.6325	<0.0001
2dpl-IVweek	0.6485	<0.0001	1	<0.0001
Iweek-IIweek	0.9388	0.8388	0.9628	0.0007
Iweek-IIIweek	0.9988	0.0474	0.9907	<0.0001
Iweek-IVweek	0.9467	<0.0001	1	0.0003
IIweek-IIIweek	1	0.941	1	0.996
IIweek-IVweek	1	<0.0001	0.8483	1
IIIweek-IVweek	1	0.0037	0.9363	0.9997

Table 1. Repeated-measure ANCOVA analysis followed by post-hoc pairwise comparisons for Schallert asymmetry index values.

Pairwise comparison	p (Tukey) Amplitude	p (Tukey) Slope
Stroke-Sham	3.81E-04	0.00162
Optostim-Sham	1.18E-04	0.00391
Optostim-Stroke	0.98967	0.99658
Robot-Sham	1.24E-05	7.11E-05
Robot-Stroke	0.99013	0.9928
Robot-Optostim	0.99999	0.91982
OR-Sham	0.98981	0.93768
OR-Stroke	0.00286	0.01952
OR-Optostim	9.73E-04	0.04139
OR-Robot	2.15E-04	0.00224

Table 2. One-way ANOVA pairwise comparison followed by post hoc Tukey test for calcium transient analysis

Ipsilateral GAP43 expression	p (Tukey)
Optostim-Stroke	0.51859
Robot-Stroke	0.71226
Robot-Optostim	0.95571
OR-Stroke	0.00157
OR-Optostim	0.02439
OR-Robot	0.00396

Ipsilateral PV expression	p (Tukey)
Optostim-Stroke	0.33704
Robot-Stroke	0.05077
Robot-Optostim	0.71806
OR-Stroke	4.67E-04
OR-Optostim	0.00683
OR-Robot	0.0195

Contralateral GAP43 expression	p (Tukey)
Optostim-Stroke	0.54935
Robot-Stroke	0.97618
Robot-Optostim	0.28263
OR-Stroke	0.77699
OR-Optostim	0.99871
OR-Robot	0.56041

Contralateral PV expression	p (Tukey)
Optostim-Stroke	0.88375
Robot-Stroke	0.99954
Robot-Optostim	0.88929
OR-Stroke	0.97889
OR-Optostim	0.68271
OR-Robot	0.94543

GAP43 labeled fibers	p (Tukey)
Optostim-Stroke	0.04008
Robot-Stroke	0.01097
Robot-Optostim	0.99304
OR-Stroke	7.40E-04
OR-Optostim	0.12075
OR-Robot	0.09068

Table 3. One-way ANOVA pairwise comparison followed by post hoc Tukey test for immunohistochemical analysis

Bibliography

1. Schwab ME. How hard is the CNS hardware? *Nat Neurosci.* 2010;13(12):1444-1446.

2. Dancause N, Nudo RJ. Shaping plasticity to enhance recovery after injury. *Prog Brain Res.* 2011;192:273-295.
3. Murphy TH, Corbett D. Plasticity during stroke recovery: from synapse to behaviour. *Nat Rev Neurosci.* 2009;10(12):861-872.
4. Zeiler SR, Krakauer JW. The interaction between training and plasticity in the poststroke brain. *Curr Opin Neurol.* 2013;26(6):609-616.
5. Takatsuru Y, Fukumoto D, Yoshitomo M, Nemoto T, Tsukada H, Nabekura J. Neuronal circuit remodeling in the contralateral cortical hemisphere during functional recovery from cerebral infarction. *J Neurosci.* 2009;29(32):10081-10086.
6. Iwai M, Stetler RA, Xing J, et al. Enhanced oligodendrogenesis and recovery of neurological function by erythropoietin after neonatal hypoxic/ischemic brain injury. *Stroke.* 2010;41(5):1032-1037.
7. Zhao Y, Rempe DA. Targeting astrocytes for stroke therapy. *Neurotherapeutics.* 2010;7(4):439-451.
8. Boyden ES, Zhang F, Bamberg E, Nagel G, Deisseroth K. Millisecond-timescale, genetically targeted optical control of neural activity. *Nat Neurosci.* 2005;8(9):1263-1268.
9. Li N, Daie K, Svoboda K, Druckmann S. Robust neuronal dynamics in premotor cortex during motor planning. *Nature.* 2016;532(7600):459-464.
10. Yizhar O, Fenno LE, Davidson TJ, Mogri M, Deisseroth K. Optogenetics in neural systems. *Neuron.* 2011;71(1):9-34.
11. Wahl AS, Buchler U, Brandli A, et al. Optogenetically stimulating intact rat corticospinal tract post-stroke restores motor control through regionalized functional circuit formation. *Nat Commun.* 2017;8(1):1187.
12. Murase N, Duque J, Mazzocchio R, Cohen LG. Influence of interhemispheric interactions on motor function in chronic stroke. *Ann Neurol.* 2004;55(3):400-409.
13. Volz LJ, Vollmer M, Michely J, Fink GR, Rothwell JC, Grefkes C. Time-dependent functional role of the contralesional motor cortex after stroke. *Neuroimage Clin.* 2017;16:165-174.
14. Cheng MY, Wang EH, Woodson WJ, et al. Optogenetic neuronal stimulation promotes functional recovery after stroke. *Proc Natl Acad Sci U S A.* 2014;111(35):12913-12918.
15. Tennant KA, Taylor SL, White ER, Brown CE. Optogenetic rewiring of thalamocortical circuits to restore function in the stroke injured brain. *Nat Commun.* 2017;8:15879.
16. Alia C, Spalletti C, Lai S, et al. Neuroplastic Changes Following Brain Ischemia and their Contribution to Stroke Recovery: Novel Approaches in Neurorehabilitation. *Front Cell Neurosci.* 2017;11:76.
17. Straudi S, Martinuzzi C, Baroni A, et al. Monitoring Step Activity During Task-Oriented Circuit Training in High-Functioning Chronic Stroke Survivors: A Proof-of-Concept Feasibility Study. *Ann Rehabil Med.* 2016;40(6):989-997.
18. Graef P, Dadalt MLR, Rodrigues D, Stein C, Pagnussat AS. Transcranial magnetic stimulation combined with upper-limb training for improving function after stroke: A systematic review and meta-analysis. *J Neurol Sci.* 2016;369:149-158.
19. Hosomi K, Morris S, Sakamoto T, et al. Daily Repetitive Transcranial Magnetic Stimulation for Poststroke Upper Limb Paresis in the Subacute Period. *J Stroke Cerebrovasc Dis.* 2016;25(7):1655-1664.
20. Edwards DJ. On the understanding and development of modern physical neurorehabilitation methods: robotics and non-invasive brain stimulation. *J Neuroeng Rehabil.* 2009;6:3.
21. Edwards DJ, Krebs HI, Rykman A, et al. Raised corticomotor excitability of M1 forearm area following anodal tDCS is sustained during robotic wrist therapy in chronic stroke. *Restor Neurol Neurosci.* 2009;27(3):199-207.
22. Triccas LT, Burridge JH, Hughes A, Verheyden G, Desikan M, Rothwell J. A double-blinded randomised controlled trial exploring the effect of anodal transcranial direct current stimulation and uni-lateral robot therapy for the impaired upper limb in sub-acute and chronic stroke. *NeuroRehabilitation.* 2015;37(2):181-191.

23. Simonetti D, Zollo L, Milighetti S, et al. Literature Review on the Effects of tDCS Coupled with Robotic Therapy in Post Stroke Upper Limb Rehabilitation. *Front Hum Neurosci.* 2017;11:268.
24. Dana H, Chen TW, Hu A, et al. Thy1-GCaMP6 transgenic mice for neuronal population imaging in vivo. *PLoS One.* 2014;9(9):e108697.
25. Pasquini M, Lai S, Spalletti C, et al. A Robotic System for Adaptive Training and Function Assessment of Forelimb Retraction in Mice. *IEEE Trans Neural Syst Rehabil Eng.* 2018;26(9):1803-1812.
26. Spalletti C, Lai S, Mainardi M, et al. A robotic system for quantitative assessment and poststroke training of forelimb retraction in mice. *Neurorehabil Neural Repair.* 2014;28(2):188-196.
27. Conti E, Allegra Mascaro AL, Pavone FS. Large Scale Double-Path Illumination System with Split Field of View for the All-Optical Study of Inter-and Intra-Hemispheric Functional Connectivity on Mice. *Methods Protoc.* 2019;2(1).
28. Crocini C, Ferrantini C, Coppini R, et al. Optogenetics design of mechanistically-based stimulation patterns for cardiac defibrillation. *Sci Rep.* 2016;6:35628.
29. Turrini L, Fornetto C, Marchetto G, et al. Optical mapping of neuronal activity during seizures in zebrafish. *Sci Rep.* 2017;7(1):3025.
30. Cecchini G, Scaglione A, Allegra Mascaro AL, et al. Cortical propagation tracks functional recovery after stroke. *PLoS Comput Biol.* 2021;17(5):e1008963.
31. Allegra Mascaro AL, Conti E, Lai S, et al. Combined Rehabilitation Promotes the Recovery of Structural and Functional Features of Healthy Neuronal Networks after Stroke. *Cell Rep.* 2019;28(13):3474-3485 e3476.
32. Spalletti C, Alia C, Lai S, et al. Combining robotic training and inactivation of the healthy hemisphere restores pre-stroke motor patterns in mice. *Elife.* 2017;6.
33. Paxinos G, Franklin KBJ. The Mouse Brain in Stereotaxic Coordinates. 1997.
34. Carmichael ST, Archibeque I, Luke L, Nolan T, Momiy J, Li S. Growth-associated gene expression after stroke: evidence for a growth-promoting region in peri-infarct cortex. *Exp Neurol.* 2005;193(2):291-311.
35. Carmichael ST. Plasticity of cortical projections after stroke. *Neuroscientist.* 2003;9(1):64-75.
36. Carmichael ST. Cellular and molecular mechanisms of neural repair after stroke: making waves. *Ann Neurol.* 2006;59(5):735-742.
37. Li S, Carmichael ST. Growth-associated gene and protein expression in the region of axonal sprouting in the aged brain after stroke. *Neurobiol Dis.* 2006;23(2):362-373.
38. Schaden H, Stuermer CA, Bahr M. GAP-43 immunoreactivity and axon regeneration in retinal ganglion cells of the rat. *J Neurobiol.* 1994;25(12):1570-1578.
39. Benowitz LI, Routtenberg A. GAP-43: an intrinsic determinant of neuronal development and plasticity. *Trends Neurosci.* 1997;20(2):84-91.
40. DiFiglia M, Roberts RC, Benowitz LI. Immunoreactive GAP-43 in the neuropil of adult rat neostriatum: localization in unmyelinated fibers, axon terminals, and dendritic spines. *J Comp Neurol.* 1990;302(4):992-1001.
41. Sakadzic S, Lee J, Boas DA, Ayata C. High-resolution in vivo optical imaging of stroke injury and repair. *Brain Res.* 2015;1623:174-192.
42. Cheng MY, Aswendt M, Steinberg GK. Optogenetic Approaches to Target Specific Neural Circuits in Post-stroke Recovery. *Neurotherapeutics.* 2016;13(2):325-340.
43. Montagni E, Resta F, Mascaro ALA, Pavone FS. Optogenetics in Brain Research: From a Strategy to Investigate Physiological Function to a Therapeutic Tool. *Photonics.* 2019;6(3):92.
44. Pendharkar AV, Levy SL, Ho AL, Sussman ES, Cheng MY, Steinberg GK. Optogenetic modulation in stroke recovery. *Neurosurg Focus.* 2016;40(5):E6.
45. Bauer AQ, Kraft AW, Wright PW, Snyder AZ, Lee JM, Culver JP. Optical imaging of disrupted functional connectivity following ischemic stroke in mice. *Neuroimage.* 2014;99:388-401.

46. Song M, Yu SP, Mohamad O, et al. Optogenetic stimulation of glutamatergic neuronal activity in the striatum enhances neurogenesis in the subventricular zone of normal and stroke mice. *Neurobiol Dis.* 2017;98:9-24.
47. Butefisch CM. Neurobiological bases of rehabilitation. *Neurol Sci.* 2006;27 Suppl 1:S18-23.
48. Jinno S, Kosaka T. Parvalbumin is expressed in glutamatergic and GABAergic corticostriatal pathway in mice. *J Comp Neurol.* 2004;477(2):188-201.
49. Lee AT, Vogt D, Rubenstein JL, Sohal VS. A class of GABAergic neurons in the prefrontal cortex sends long-range projections to the nucleus accumbens and elicits acute avoidance behavior. *J Neurosci.* 2014;34(35):11519-11525.
50. Rock C, Zurita H, Lebby S, Wilson CJ, Apicella AJ. Cortical Circuits of Callosal GABAergic Neurons. *Cereb Cortex.* 2018;28(4):1154-1167.
51. Swanson OK, Maffei A. From Hiring to Firing: Activation of Inhibitory Neurons and Their Recruitment in Behavior. *Front Mol Neurosci.* 2019;12:168.
52. Lai S, Panarese A, Spalletti C, et al. Quantitative kinematic characterization of reaching impairments in mice after a stroke. *Neurorehabil Neural Repair.* 2015;29(4):382-392.